Psychological Review, 1988, **95**, 49–90

CHAPTER 13
NEURAL DYNAMICS OF PLANNED ARM MOVEMENTS: EMERGENT INVARIANTS AND SPEED-ACCURACY PROPERTIES DURING TRAJECTORY FORMATION

Daniel Bullock† and Stephen Grossberg‡

Abstract

A real-time neural network model, called the Vector Integration to Endpoint, or VITE, Model, is developed and used to quantitatively simulate behavioral and neural data about planned and passive arm movements. Invariants of arm movements emerge through network interactions rather than through an explicitly precomputed trajectory. Motor planning occurs in the form of a Target Position Command, or TPC, which specifies where the arm intends to move, and an independently controlled GO command, which specifies the movement's overall speed. Automatic processes convert this information into an arm trajectory with invariant properties. These automatic processes include computation of a Present Position Command, or PPC, and a Difference Vector, or DV. The DV is the difference of the PPC and the TPC at any time. The PPC is gradually updated by integrating the DV through time. The GO signal multiplies the DV before it is integrated by the PPC. The PPC generates an outflow movement command to its target muscle groups. Opponent interactions regulate the PPC's to agonist and antagonist muscle groups. This system generates synchronous movements across synergetic muscles by automatically compensating for the different total contractions that each muscle group must undergo. Quantitative simulations are provided of Woodworth's Law, of the speed-accuracy trade-off known as Fitts' Law, of isotonic arm movement properties before and after deafferentation, of synchronous and compensatory "central error correction" properties of isometric contractions, of velocity amplification during target switching, of velocity profile invariance and asymmetry, of the changes in velocity

† Supported in part by the National Science Foundation (NSF IST-84-17756).

‡ Supported in part by the Air Force Office of Scientific Research (AFOSR F49620-86-C-0037 and AFOSR F49620-87-C-0018) and the National Science Foundation (NSF IST-84-17756).

profile asymmetry at higher movement speeds, of the automatic compensation for staggered onset times of synergetic muscles, of vector cell properties in precentral motor cortex, of the inverse relationship between movement duration and peak velocity, and of peak acceleration as a function of movement amplitude and duration. It is shown that TPC, PPC, and DV computations are needed to actively modulate, or gate, the learning of associative maps between TPC's of different modalities, such as between the eye-head system and the hand-arm system. By using such an associative map, looking at an object can activate a TPC of the hand-arm system, as Piaget noted. Then a VITE circuit can translate this TPC into an invariant movement trajectory. An auxiliary circuit, called the Passive Update of Position, or PUP, Model, is described for using inflow signals to update the PPC during passive arm movements due to external forces. Other uses of outflow and inflow signals are also noted, such as for adaptive linearization of a nonlinear muscle plant, and sequential read-out of TPC's during a serial plan, as in reaching and grasping. Comparisons are made with other models of motor control, such as the mass-spring and minimum-jerk models.

13.1. Introduction: Are Movement Invariants Explicitly Planned?

The subjective ease with which we carry out simple action plans—rotating a wrist-watch into view, lifting a coffee cup, or making a downstroke while writing—masks the enormously complex integrative apparatus needed to achieve and maintain coordination among the thousands of sensors, neurons, and skeleto-motor units that contribute to any act's planning and execution. Moreover, recent studies of the kinematics of planned arm movements (Abend, *et al.*, 1982; Atkeson and Hollerbach, 1985; Howarth and Beggs, 1981) have shown that the integrative action of all these separate contributors produces velocity profiles whose global shape is remarkably invariant over a wide range of movement sizes and speeds. This raises a fundamental question for the theory of sensory-motor control, and for the neurosciences in general: How can the integrated activity of thousands of separate elements produce globally invariant properties?

Two broad species of answers to this question can be contemplated. The first includes theories that posit the existence of a high level stage involving explicit computation and internal representation of the invariant, in this case the velocity profile, as a whole. This representation is then used as a basis for performing the desired action. Such theories have been favored recently by many workers in the field of robotics, and at least one theory of this type has already been partially formulated to accommodate kinematic data on human movements: the "minimized Cartesian jerk theory" (Hogan, 1984; Flash and Hogan, 1985), which is a special case of global optimization analysis. The second species of answers includes theories in which no need arises for explicit computation and representation of the invariant trajectory as a whole (Sections 13.7 and 13.16). In models

associated with such theories, a trajectory with globally invariant properties emerges in real-time as the result of events distributed across many interacting sensory, neural, and muscular loci.

This article describes a theory of arm trajectory invariants that conforms to the latter ideal (Bullock and Grossberg, 1986). Our analysis suggests that trajectory invariants are best understood not by focusing on velocity profiles as such, but by pursuing more fundamental questions: What principles of adaptive behavioral organization constrain the system design that governs planned arm movements? What mechanisms are needed to realize these principles as a real-time neural network? Our development of this topic proceeds via analyses of learned eye-hand coordination, synchronization among synergists, intermediate position control during movement, and variable velocity control. These analyses disclose a neural network design whose qualitative and quantitative operating characteristics match those observed in a wide range of experiments on human movement. Because velocity profile invariance, as well as speed-dependent changes in velocity profile asymmetry ignored by prior models (Section 13.12), are among the neural network's emergent operating characteristics, our work shows that neither an explicit trajectory nor a kinematic invariant need be explicitly represented within a motor control system at any time. Thus our work supports a critical insight of workers in the mass-spring modeling tradition, that movement kinematics need not be explicitly pre-programmed. By the same token, our results reject a mass-spring model in its customary form and argue against models based upon optimization theory. Instead we show how a movement control system may be adaptive without necessarily optimizing an explicit cost function.

To further support these conclusions, we use the neural model to quantitatively simulate Woodworth's Law and Fitts' Law, the empirically derived speed-accuracy tradeoff function relating error magnitudes, movement distances and movement durations; isotonic arm movement properties before and after deafferentation (Bizzi, Accornero, Chapple, and Hogan, 1982, 1984; Evarts and Fromm, 1978; Polit and Bizzi, 1978); synchronous and compensatory "central error correction" properties of isometric contractions (Freund and Büdingen, 1978; Ghez and Vicario, 1978; Gordon and Ghez, 1984, 1987a, 1987b,); velocity amplification during target switching (Georgopoulos, Kalaska, and Massey, 1981); velocity profile invariance and asymmetry (Abend, Bizzi, and Morasso, 1982; Atkeson and Hollerbach, 1985; Georgopoulos, Kalaska, and Massey, 1981; Beggs and Howarth, 1972; Morasso, 1981; Soechting and Lacquaniti, 1981); the changes in velocity profile asymmetry at higher movement speeds (Beggs and Howarth, 1972; Zelaznik, Schmidt, and Gielen, in press); vector cell properties in precentral motor cortex (Evarts and Tanji, 1974; Georgopoulos, Kalaska, Caminiti, and Massey, 1982; Georgopoulos, Kalaska, Crutcher, Caminiti, and Massey, 1984; Kalaska, Caminiti, and Georgopoulos, 1983; Tanji and Evarts, 1976); the inverse relationship between movement duration and peak velocity (Lestienne, 1979); and peak acceleration as a function of movement amplitude and time (Bizzi, Accornero, Chapple, and Hogan, 1984). In addition, the work reported here extends a broader

program of research on adaptive sensory-motor control (Grossberg, 1978a, 1986a, 1986b; Grossberg and Kuperstein, 1986), which enables functional and mechanistic comparisons to be made between the neural systems governing arm and eye movements, suggests how eye-hand coordination is accomplished, and provides a foundation for work on mechanisms of trajectory realization which compensate for the mechanical effects generated by variable loads and movement velocities (Bullock and Grossberg, 1988b).

13.2. Flexible Organization of Muscle Groups into Synergies

In order to move a part of the body, whether an eye, head, arm, or leg, many muscles must work together. For example, muscles controlling several different joints—shoulder, elbow, wrist, and fingers—may contract or relax cooperatively in order to perform a reaching movement. When groups of muscles cooperate in this way, they are said to form a synergy (Bernstein, 1967; Kelso, 1982).

Muscle groups may be incorporated into synergies in a flexible and dynamic fashion. Whereas muscles controlling shoulder, elbow, wrist, and fingers may all contract or relax synergetically to produce a reaching movement, muscles of the fingers and wrist may form a synergy to perform a grasping movement. Thus, one synergy may activate shoulder, elbow, wrist, and finger muscles to reach towards an object, and another synergy may then activate only finger and wrist muscles to grasp the object while maintaining postural control over the shoulder and elbow muscles. Groups of fingers may move together synergetically to play a chord on the piano, or separate fingers may be successively activated in order to play arpeggios.

One of the basic problems of motor control is to understand how neural control structures quickly and flexibly reorganize the set of muscle groups that are needed to synergetically cooperate in the next movement sequence. Once one squarely faces the problem that many behaviorally important synergies are not hard-wired, but are rather dynamically coupled and decoupled through time in ways that depend upon the actor's experience and training, the prospect that the trajectories of all synergists are explicitly preplanned seems remote at best. In support of a dynamic conception of synergy formation, Buchanan, Almdale, Lewis, and Rymer (1986) conclude from their experiments on isometric contractions of human elbow muscles that "The complexity of these patterns raises the possibility that synergies are determined by the tasks and may have no independent existence."

13.3. Synchronous Movement of Synergies

When neural commands organize a group of muscles into a synergy, the action of these muscles often occurs synchronously through time. It is partly for this reason that the complexity of the neural commands controlling many movements often goes unnoticed. These movements seem to occur in a single gesture, rather than as the sum of many asynchronous components.

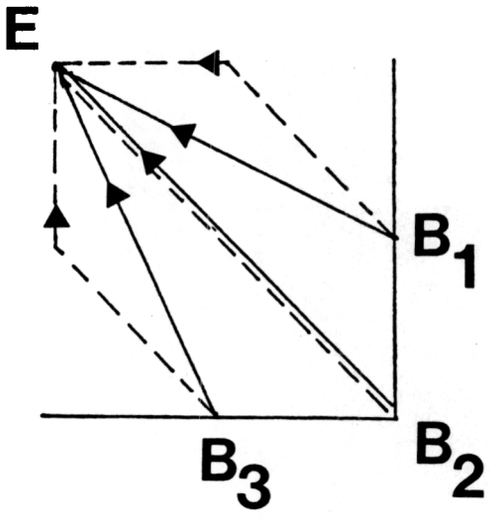

Figure 13.1. Consequences of two motor-control schemes. Dashed lines: Movement paths generated when a synergist producing vertical motion and a synergist producing horizontal motion contract in parallel and at equal rates to effect movements from various beginning points (Bs) to the common endpoint E. Solid lines: Movement paths generated when the synergists' contraction rates are adjusted to compensate for differences in the lengths of the vertical and horizontal components of the movement.

In order to understand the type of control problem that must be solved to generate synchronous movement, consider a typical arm movement of reaching forward and across the body midline with the right hand in a plane parallel to the ground. Suppose for simplicity that the synergist acting at the shoulder is responsible for across-midline motion, that the synergist acting at the elbow is responsible for forward motion, and that the hand is to be moved from points B1, B2, or B3 to point E. Figure 13.1 illustrates the effects of two distinct control schemes that might be used to produce these three movements. In the first scheme, the two synergists begin their contractions synchronously, contract at the same rate, and cease contracting when their respective motion component is complete. This typically results in asynchronous contraction terminations, and in bent-line movements, because the synergist responsible for the longer motion component takes longer to complete its contribution. With this scheme, approximately straight-line motions and synchronous contraction terminations occur only in cases like the B2–E movement, for which the component motions happen to be of equal length. In the second scheme, the two synergists contract, not at equal rates, but at rates that have been adjusted to compensate for any differences in length of the com-

ponent motions. This results in synchronous contraction terminations. Normal arm movement paths are similar to those implied by the second control scheme (e.g., Morasso, 1981) and experimental studies (Freund and Büdingen, 1978) have shown that contraction rates are made unequal in a way that compensates for inequalities of distance.

What types of adaptive problems are solved by synchronization of synergists? Figure 13.1 provides some insight into this issue. Without synchronization, the direction of the first part of the movement path may change abruptly several times before the direction of the last part of the movement path is generated (Figure 13.1). This creates a problem because transporting an object from one place to another with the arm may destabilize the body unless one can predict, and anticipatorily compensate for, the arm movement's destabilizing effects, which are always directional. In the same way, many actions require that forces be applied to surfaces in particular directions. The first control scheme makes the direction in which force is applied difficult to predict and control. Both of these problems are eliminated by the approximately straight-line movement paths which become possible when synergists contract synchronously. Finally, if the various motions composing a movement failed to end synchronously, it would become difficult to ensure smooth transitions between sequentially ordered movements.

In summary, the untoward effects of asynchrony place strong constraints on the mechanisms of movement control: Across the set of muscles whose synergistic action produces a multi-joint movement, contraction durations must be roughly equal, and, because contraction distances are typically unequal, contraction rates must be made unequal in a way that compensates for inequalities of distance.

13.4. Factoring Target Position and Velocity Control

Inequalities of distance are translated into neural commands as differences in the total amounts of contraction by the muscles forming the synergy, and thereby into mechanical terms as the total amounts of change in the angles between joints (Hollerbach, Moore, and Atkeson, 1986). In order to compensate for differences in contraction, information must be available that is sufficient to compute the total amounts of contraction that are required. Thus a representation of the initial contraction level of each muscle must be compared with a representation of the target, expected, or final contraction level of the muscle. A primary goal of this article is to specify how this comparison is made. Although information about target position and initial position are both needed to control the total contraction of a muscle group, these two types of information are computed and updated in different ways, a fact that we believe has caused much confusion about whether only target position needs to be coded (Section 13.7). In particular, we reject the common assumption (Adams, 1971) that the representation of initial contraction used in the comparison is based on afferent feedback from the limbs. We propose instead that it is based primarily on feedback from an outflow command integrator that is located

along the pathway between the precentral motor cortex and the spinal motorneurons.

Another source of confusion has arisen because target position information is needed to form a trajectory. This is the type of information which invites concepts of motor planning and expectation. However tempting it may be to so infer, concepts of motor planning and expectation do *not* imply that the *whole trajectory* is *explicitly* planned.

A second aspect of planning enters into trajectory formation which also does not imply the existence of explicit trajectory planning. This aspect is noticed by considering that the hand-arm system can be moved between fixed intital and target positions at many different velocities. When, as a result of a changed velocity, the overall movement duration changes, the component motions occurring around the various joints must nonetheless remain synchronous. Since fixed differences in initial and target positions can be converted into synchronous motions at a wide range of velocities, there must exist an independently controlled velocity, or GO signal (Section 13.11). The independent control of target position commands, or TPCs, and velocity commands, or GO signals, is a special case of a general neural design which has been called the *factorization of pattern and energy* (Grossberg, 1978a, 1982a).

13.5. Synchrony versus Fitts' Law: The Need for a Neural Analysis of Synergy Formation

Our discussion of synchronous performance of synergies has thus far emphasized that different muscles of the hand-arm system may need to contract by different amounts in equal time in order to move a hand through a fixed distance. When movement of a hand over different distances is considered, a striking contrast between behavioral and neural properties of movement becomes evident. This difference emphasizes that synergies are assembled and disassembled through time in a flexible and dynamic way.

Fitts' Law (Fitts, 1954; Fitts and Peterson, 1964) states that movement time (MT) of the arm is related to distance moved (D) and to width of target (W) by the equation

$$MT = a + b\log_2(\frac{2D}{W}), \tag{13.1}$$

where a and b are empirically derived constants. Keele (1981) has reviewed a variety of experiments showing that Fitts' Law is remarkably well obeyed despite its simplicity. For example, the law describes movement time for linear arm movements (Fitts, 1954), rotary movements of the wrist (Knight and Dagnall, (1967), back-and-forth movements like dart throwing (Kerr and Langolf, 1977), head movements (Jagacinski and Monk, 1985), movements of young and old people (Welford, Norris, and Schock, 1969), and movements of monkeys as well as humans (Brooks, 1979).

Equation (13.1) asserts that movement time (MT) increases as the logarithm of distance (D) moved, other things being equal. The width parameter W in (13.1) is interpreted as a measure of movement accuracy (Section 13.27). Although movement distance and time may covary on the behavioral level that describes the aggregate effect of many muscle contractions, such a relationship does not necessarily hold on the neural level, where individual muscles may contract by variable amounts, or "distances", in order to achieve synchronous contraction within a constant movement time.

A fundamental issue is raised by this comparison of behavioral and neural constraints. This issue can be better understood through consideration of the following gedanken example. When each of two fingers is moved separately through different distances, each finger may separately obey Fitts' Law. Then the finger which moves a larger distance should take more time to move, other things being equal. In contrast, when the two fingers move the above distances as part of a single synergy, then each finger should complete its movement in the same time in order to guarantee synergetic synchrony. Thus either one of the fingers must violate Fitts' Law, or it must reach its target with a different level of accuracy. Kelso, Southard, and Goodman (1979) and Marteniuk and MacKenzie (1980) have experimentally studied this type of synchronous behavior in experiments on one or two handed movements, and have documented within-synergy violations of Fitts' Law.

Such examples suggest that Fitts' Law holds for the aggregate behavior of the largest collection of motor units which form a synergy during a given time interval. Fitts' Law need not hold for all subsets of the motor units which comprise a synergy. These subsets may, in principle, violate Fitts' Law by travelling variable distances in equal time in order to achieve synchrony of the aggregate movement. To understand how Fitts' Law can be reconciled with movement synchrony thus requires an analysis of the neural control mechanisms which flexibly bind muscle groups, such as those controlling different fingers, into a single motor synergy. If such a binding action does not involve explicit planning of a complete trajectory, yet does require activation of a target position command and a GO command, then neural machinery must exist which is capable of *automatically* coverting such commands into complete trajectories with synchronous and invariant properties. One of the primary tasks of this article is to describe the circuit design of this neural machinery and to explain how it works.

13.6. Some General Issues in Sensory-Motor Planning: Multiple Uses of Outflow versus Inflow Signals

Before beginning a mechanistic analysis of these circuits, we summarize several general issues about motor planning to place the model developed in this article within a broader conceptual framework. In Sections 13.8–13.13 and 13.27–13.29, a number of key experiments are reviewed to more sharply constrain the theoretical analysis. In Sections 13.21–13.28 computer simulations of these data properties are reported.

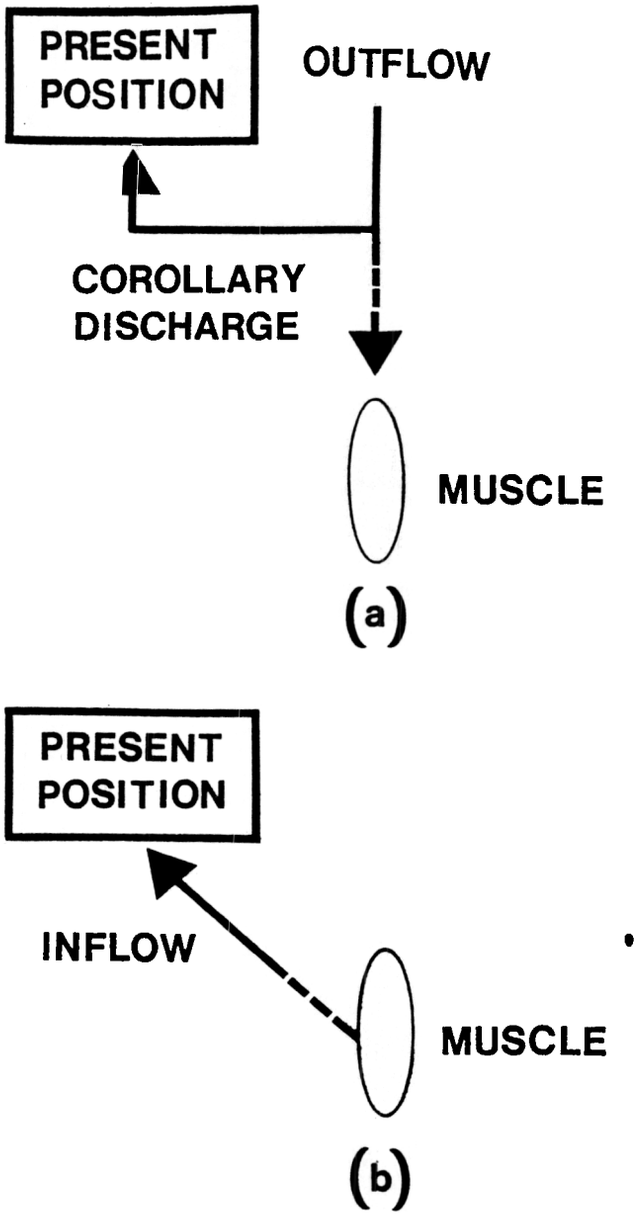

Figure 13.2. Both outflow and inflow signals contribute to the brain's estimate of the limb's present position, but in different ways.

Neural circuitry automates the production of skilled movements in several mechanistically distinct ways. Perhaps the most general observation is that animals and humans perform marvelously dexterous acts in a world governed by Newton's Laws, yet can go through life without ever learning Newton's Laws, and indeed may have a great deal of difficulty learning them when they try. The phenomenal world of movements is a world governed by motor plans and intentions, rather than by kinematic and inertial laws. A major challenge to theories of biological movement control is to explain how we move so well within a world whose laws we may so poorly understand.

The computation of a hand or arm's present position illustrates the complexity of this problem. Two general types of present position signals have been identified in discussions of motor control: *outflow* signals and *inflow* signals. Figure 13.2 schematizes the difference between these signal sources. An outflow signal carries a movement command from the brain to a muscle (Figure 13.2a). Signals that branch off from the efferent brain-to-muscle pathway in order to register present position signals are called *corollary discharges* (Helmholtz, 1866; von Holst and Mittelstaedt, 1950). An *inflow* signal carries present position information from a muscle to the brain (Figure 13.2b). A primary difference between outflow and inflow is that a change in outflow signals is triggered only when an observer's brain generates a new movement command. A new inflow signal can, in contrast, be generated by passive movements of the limb. Evidence for influences of both outflow (Helmholtz, 1866) and inflow (Ruffini, 1898; Sherrington, 1894) has accumulated over the past century. Disentangling the different roles played by outflow and inflow signals has remained one of the major problems in motor control. This is a confusing issue because both outflow and inflow signals are used in multiple ways to provide different types of information about present position. The following summary itemizes some of the ways in which these signals are used in our theory.

Although one role of an outflow signal is to move a limb by contracting its target muscles, the operating characteristics of the muscle plant are not known *a priori* to the outflow source. It is therefore not known *a priori* how much the muscle will actually contract in response to an outflow signal of prescribed size. It is also not known how much the limb will move in response to a prescribed muscle contraction. In addition, even if the outflow system somehow possessed this information at one time, it might turn out to be the wrong information at a later time, because muscle plant characteristics can change through time due to development, aging, exercise, changes in blood supply, or minor tears. Thus the relationship between the size of an outflow movement command and the amount of muscle contraction is, in principle, undeterminable without additional information which characterizes the muscle plant's actual response to outflow signals.

To establish a satisfactory correspondence between outflow movement signals and actual muscle contractions, the motor system needs to compute reliable present position signals which represent where the outflow command tells the muscle to move, as well as reliable present position signals which represent the state of contraction of the muscle. Corollary

discharges and inflow signals can provide these different types of information. Grossberg and Kuperstein (1986) have shown how a comparison, or match, between corollary discharges and inflow signals can be used to modify, through an automatic learning process, the total outflow signal to the muscle in a way that effectively compensates for changes in the muscle plant. Such automatic gain control produces a linear correspondence between an outflow movement command and the amount of muscle contraction even if the muscle plant is nonlinear. The process which matches outflow and inflow signals to linearize the muscle plant response through learning is called *adaptive linearization* of the muscle plant. The cerebellum is implicated by both the theoretically derived circuit and experimental evidence as the site of learning (Albus, 1971; Brindley, 1964; Fujita, 1982a, 1982b; Grossberg, 1969a, 1972a; Ito, 1974, 1982, 1984; Marr, 1969; McCormick and Thompson, 1984; Optican and Robinson, 1980; Ron and Robinson, 1973; Vilis and Hore, 1986; Vilis, Snow, and Hore, 1983).

Given that corollary discharges are matched with inflow signals to linearize the relationship between muscle plant contraction and outflow signal size, outflow signals can also be used in yet other ways to provide information about present position. In Sections 13.17–13.23, it is shown how outflow signals are matched with target position signals to generate a trajectory with synchronous and invariant properties. Thus outflow signals are used in at least three ways, and all of these ways are automatically registered: They send movement signals to target muscles; they generate corollary discharges which are matched with inflow signals to guarantee linear muscle contractions even if the muscle plant is nonlinear; and they generate corollary discharges which are matched with target position signals to generate synchronous trajectories with invariant properties.

Inflow signals are also used in several ways. One way has already been itemized. A second use of inflow signals is suggested by the following gedanken example. When you are sitting in an armchair, let your hands drop passively towards your sides. Depending upon a multitude of accidental factors, your hands and arms can end up in any of infinitely many final positions. If you are then called upon to make a precise movement with your arm-hand system, this can be done with the usual exquisite accuracy. Thus the fact that your hands and arms start out this movement from an initial position which was not reached under active control by an outflow signal does not impair the accuracy of the movement.

A wealth of evidence suggests, however, that comparison between target position and present position information is used to move the arms. Moreover, as will be shown below, this present position information is computed from outflow signals. In contrast, during the passive fall of an arm under the influence of gravity, changes in outflow signal commands are not responsible for the changes in position of the limb. This observation identifies the key issue: How is the outflow signal updated due to passive movement of a limb so that the next active movement can accurately be made? Since the final position of a passively falling limb cannot be predicted in advance, it is clear that inflow signals must be used to update present position when an arm is moved passively by an external

force.

This conclusion calls attention to a closely related issue that must be dealt with to understand the neural bases of skilled movement: How does the motor system know that the arm is being moved passively due to an external force, and not actively due to a changing outflow command? Such a distinction is needed to prevent inflow information from contaminating outflow commands when the arm is being actively moved. The motor system must use internally generated signals to make the distinction between active movement and passive movement, or postural, conditions. Computational gates must be open and shut based upon whether these internally generated signals are on or off (Grossberg and Kuperstein, 1986).

A third role for inflow signals is needed due to the fact that arms can move at variable velocities while carrying variable loads. Because an arm is a mechanical system embedded in a Newtonian world, an arm can generate unexpected amounts of inertia and acceleration when it tries to move novel loads at novel velocities. During such a novel motion, the commanded outflow position of the arm and its actual position may significantly diverge. Inflow signals are needed to compute mismatches leading to partial compensation for this uncontrolled component of the movement.

Such novel movements are quite different from our movements when we pick up a familiar fountain pen or briefcase. When the object is familiar, we can predictively adjust the gain of the movement to compensate for the expected mass of the object. This type of automatic gain control can, moreover, be flexibly switched on and off using signal pathways that can be activated by visual recognition of a familiar object. Inflow signals are used in the learning process which enables such automatic gain control signals to be activated in an anticipatory fashion in response to familiar objects (Bullock and Grossberg, 1988b).

This listing of multiple uses for outflow and inflow signals invites comparison between how the arm movement system and other movement systems use outflow and inflow signals. Grossberg and Kuperstein (1986) have identified and suggested neural circuit solutions to analogous problems of sensory-motor control within the specialized domain of the saccadic eye movement system. Several of the problems to which we will suggest circuit solutions in our articles on arm movements have analogs with the saccadic circuits developed by Grossberg and Kuperstein (1986). Together these investigations suggest that several movement systems contain neural circuits that solve similar general problems. Differences between these circuits can be traced to functional specializations in the way these movement systems solve their shared problems of movement.

For example, whereas saccades are ballistic movements, arm movements can be made under both continuous and ballistic control. Whereas the eyes normally come to rest in a head-centered position, the arms can come to rest in any of infinitely many positions. Whereas the eyes are typically not subjected to unexpected or variable external loads, the arms are routinely subjected to such loads. Whereas the eyes typically generate

a stereotyped velocity profile between a fixed pair of initial and target positions, the arms can move with a continuum of velocity profiles between a fixed pair of initial and target positions. Our analyses show how the arm system is specialized to cope with all of these differences between its behaviors and those of the saccadic eye movement system.

13.7. Neural Control of Arm Position Changes: Beyond the STE Model

A number of further specialized constraints on the mechanisms controlling planned arm movements are clarified by summarizing shortcomings of the simplest example of a "mass-sping" model of movement generation, which we will call the Spring-To-Endpoint (STE) model, to distinguish it from other members of the potentially large family of models that exploit "mass-spring" properties of biological limbs (e.g., Bizzi, 1980; Cooke, 1980; Feldman, 1974, 1986; Humphrey and Reed, 1983; Kelso and Holt, 1980; Sakitt, 1980). As Nichols (1985) and Feldman (1986) have recently noted, past discussions of mass-spring properties have mistakenly lumped together quite different proposals regarding how such properties might be exploited during trajectory formation. Our treatment in this section is meant to serve a pedagogical function, and our criticisms pertain only to the STE Model which is explicitly specified in this section. In particular, no part of our critique denies that the peripheral motor system has mass-spring properties that may be critical to overall motor function. Indeed, in Bullock and Grossberg (1988b), we analyse neural command circuits which exploit mass-spring muscle properties to generate well-controlled movements.

The components of the STE (Spring-To-Endpoint) Model for movement control can be summarized as follows. Imagine that the eye fixates some object that lies within reach. To touch the object, it is necessary to move the tip of the index finger from its current position to the target position on the object's nearest surface. The STE Model suggests that this is accomplished by simply replacing the arm position command that specifies the arm's present posture with a new arm position command that specifies the posture the arm would have to assume in order for the index finger to touch the chosen object surface.

Instatement of the new arm position command is suggested to generate the desired movement as follows. The arm is held in any position by balancing the muscular and other forces (e.g., gravity) that are currently acting on the limb. Instatement of a new command changes the pattern of outflow signals that contract the arm muscles. A step change in the pattern of contraction creates a force imbalance that causes the limb to spring in the direction of the larger force at a rate proportional to the force difference. The limb comes to rest when all the forces acting on it are once again balanced. Despite its elegance, the STE Model exhibits several deficiencies which highlight properties that an adequate control system needs to have. We briefly summarize two fundamental problems: (1) confounding of speed and distance control, and (2) inability to quickly terminate movement at an intermediate position.

The first problem, the speed-distance confound, follows from the dependence of movement rate on the force difference, which in turn depends on the distance between the starting and final positions. This might at first seem to be a desirable property, because it appears to compensate for different distances in the manner needed to ensure synchronization of synergists (Section 13.3). However, consider also the need to vary the speed of a fixed movement. An actor seeking to perform the same movement at a faster speed would have to follow a two-part movement plan: Early in the movement, instate a virtual target position that is well beyond the desired end point and along a line drawn from the initial through the true target position. This command will create a very large initial force imbalance and launch the limb at a high speed. Then, at some point during the movement, instate the true target position command, and let the arm coast to the final position. This example illustrates that the STE Model requires a complex and neurally implausible scheme for achieving variable speed control for movements of fixed length.

Cooke (1980) suggests that variable speed control by an STE Model can be achieved by abruptly changing the stiffness of agonist and antagonist muscles to achieve differences in distance and speed. This model has not yet been shown to produce velocity profiles with the parametric properties of the data (Section 13.12). In addition, Houk and Rymer (1981) and Feldman (1986) have shown that the stiffness of individual muscles is typically maintained at a nearly constant level.

A second problem with the STE Model concerns the critical need to quickly abort an evolving movement and stabilize current arm position. Such a need arises, for example, when an animal wishes to freeze upon detection of a predator who uses motion cues to locate prey. It also arises when an action, such as transporting a large mass, begins to destabilize an animal's overall state of balance. At such times, it is often adaptive to quickly freeze and maintain the current arm position. This is an easy task if the movement command is never much different from the arm's present position. Freezing could then be quickly achieved by preventing further changes in the currently commanded position. In an STE Model, this simple freeze strategy is unavailable, because a large discrepancy exists between present arm position and the target position command throughout much of the trajectory. To implement a freezing response using the STE Model, the system would somehow have to quickly determine and instate a new target position command capable of maintaining the arm's present position. But this is precisely the type of information whose relevance is denied by the STE Model.

13.8. Gradual Updating of PPC's during Trajectory Formation

Several lines of experimental evidence point to deficiencies of the STE Model. One line of evidence, due to Bizzi and his colleagues, demonstrates that a type of gradual updating of the movement command occurs which is inconsistent with the STE model. Earlier studies from the Bizzi lab partially supported the STE model.

The experiments of Polit and Bizzi (1978) studied monkeys who were trained to move their forearms, without visual feedback of hand position, from a canonical starting position to the position of one of several lights. The monkeys' arm movements were studied both before and after a dorsal rhizotomy was performed to remove all sensory feedback from the arm. Before deafferentation, the monkey could move its hand to the target's position without visual feedback, even if its accustomed position with respect to the arm apparatus was changed. After deafferentation, so long as the spatial conditions of training were maintained—in particular the canonical starting orientation and position with respect to the known target array—the animal remained able to move its hand to the target position. However, if the initial position of the upper arm and elbow of the deafferented arm was passively shifted from the position used throughout training, then the animal's forearm movements terminated at a position shifted by an equal amount away from the target position. Thus the movement of the forearm did not compensate for the change in initial position of the upper arm. Instead the same final synergy of forearm-controlling muscles was generated in both cases.

The fact that deafferented monkeys moved to shifted positions emphasized the critical role of the target position command in setting up the movement trajectory. The fact that normal monkeys could compensate for rotation in a way that deafferented monkeys could not indicated an additional role for inflow signals when the arm is moved passively by an external force (Section 13.29).

The later experiments of Bizzi, Accornero, Chapple, and Hogan (1982, 1984) carried out an additional manipulation. The results of these experiments are inconsistent with the STE assumption that the arm's motion is governed exclusively by the spring-like contraction of its muscles towards the position specified by a new target position command. In these experiments, the monkey was again deprived of visual and inflow feedback, and placed in its canonical starting position. In addition, its deafferented arm was surreptitiously held at the target position, then released at variable intervals after activation of the target light. Under these circumstances, the arm travelled back towards the canonical starting position, before reversing direction and proceeding to the target. The arm travelled further backward toward the starting position the sooner it was released after target activation. Moreover, when the arm was moved to the target position and then released in the absence of any target presentation, it sprang back to its canonical starting position. Bizzi *et al.* (1984, p.2742) concluded that "the CNS had programmed a slow, gradual shift of the equilibrium point, a fact which is not consistent with the 'final position control' [read STE] hypothesis."

The Bizzi *et al.* (1984) description of their results as a "gradual shift of the equilibrium point" carries the language of the STE Model into a context where it may cause confusion. From a mathematical perspective, the intermediate positions of a movement trajectory are not, by definition, equilibrium points. In order to explicate the Bizzi *et al.* (1984) data, we show how three quantities are computed and updated through time: a

target position command (TPC) which is switched on once and for all before the movement; an outflow movement command, called the present position command (PPC), which is continously updated until it matches the TPC; and the arm position which closely corresponds to the PPC. We use these concepts below to explain data from the Bizzi lab in both normal and deafferented conditions.

We call a movement for which a single TPC (target position command) is switched on before the movement begins an *elementary* movement. Once it is seen how a single TPC can cause gradual updating of the PPC (present position command), movements can also be analysed during which a sequence of TPC's is switched on, either under the control of visual feedback or from a movement planning network which can store and release sequences of TPC's from memory with the proper order and timing (Grossberg and Kuperstein, 1986).

Our analysis of how the PPC is gradually updated during an elementary movement partially supports the Bizzi *et al.* (1984) description of a "gradual shift in equilibrium point" by showing that the arm remains in approximate equilibrium with respect to the PPC, even though none of these intermediate arm positions is an equilibrium point of the system. The only equilibrium point of the system is reached when both the neural control circuit and the arm itself both reach equilibrium. That happens when the PPC matches the TPC, thereby preventing further changes in the present position command and allowing the arm to come to rest.

These conclusions refine, rather than totally contradict, the main insight of the STE Model. Instead of concluding that the arm springs to the position coded by the TPC, we suggest that the spring-like arm tracks the series of positions specified by the PPC as it approaches the TPC. This conception of trajectory formation contrasts sharply with that suggested by Brooks (1986, p.138) in response to the Bizzi data. Brooks inferred that "animals learn not only the end points and their stiffness, but also a series of intermediate equilibrium positions. In other words, they learn an internal 'reference' trajectory that determines the path to be followed and generates torques appropriately to reduce mismatch between the intended and actual events." In a similar fashion, Hollerbach (1982, p.192) suggested that we practice movements to "learn the basic torque profiles." In contrast, we suggest that the read-out of the TPC is learned, but that the gradual updating of the PPC is automatic. A number of auxiliary learning processes are also needed to update the PPC after passive movements due to an external force (Section 13.30), to adaptively linearize the response of a nonlinear muscle plant (Grossberg and Kuperstein, 1986), and to adaptively compensate for the inertial effects of variable loads and velocities (Bullock and Grossberg, 1988b). These additional learning processes enable the automatic updating of the PPC to generate controllable movements without requiring that the entire trajectory be learned.

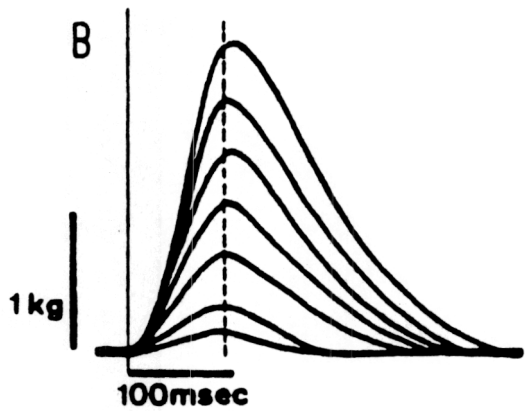

Figure 13.3. Curves for subjects' approach to various targeted force levels. Targeted (peak) levels are reached at nearly the same time, indicating duration invariance across different force "distances". Only the initial part of each curve represents active movement. Post-peak portions represent passive relaxation back to base-line. Reprinted with permission from Freund and Büdingen (1978).

13.9. Duration Invariance during Isotonic Movements and Isometric Contractions

Further information concerning the gradual updating process whereby PPC's match a TPC can be inferred from the detailed spatiotemporal properties of arm trajectory formation. Freund and Büdingen (1978) have studied "the relationship between the speed of the fastest possible voluntary contractions and their amplitudes for several hand and forearm muscles under both isotonic and isometric conditions. These experiments showed the larger the amplitude, the faster the contraction. The increase of the rate of rise of isometric tension or of the velocity of isotonic movements with rising amplitude was linear. The slope of this relationship was the same for three different hand and forearm muscles examined ... the skeleto-motor speed control system operates by adjusting the velocity of a contraction to its amplitude in such a way that the contraction time remains approximately constant ... this type of speed control is a necessary requirement for the synchrony of synergistic muscle contractions" (p.1).

Two main issues are raised by this study. First, it must be explained why, "comparing isotonic movements and isometric contractions, the time from onset to peak was similar in the two conditions" (p.7). Figure 13.3 shows the fastest voluntary isometric contractions of the extensor indicis muscle. Second, it must be explained why the force develops gradually in time with the shapes depicted in Figure 13.3. Below it is shown that both

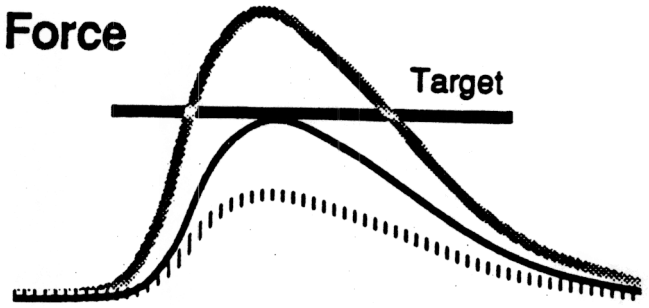

Figure 13.4. Overshooting (gray curve), hitting (black curve), and undershooting (dashed line) a force-level target (horizontal line) in an isometric task. Reprinted with permission from Gordon and Ghez (1987b).

duration invariance and the force development through time are emergent properties of the PPC updating process (see Section 13.22).

13.10. Compensatory Properties of the PPC Updating Process

Ghez and his colleagues (Ghez and Vicario, 1978; Gordon and Ghez, 1984, 1987a, 1987b) have confirmed the duration invariance reported by Freund and Büdingen (1978) in an isometric paradigm which also disclosed finer properties of the PPC updating process. These authors suggest that "compensatory adjustments add to preprogrammed specification of rapid force impulses to achieve more accurately targeted responses" (Gordon and Ghez, 1987b).

In their isometric task, subjects were instructed to maintain superposition of two lines on a CRT screen. The experimenter could cause one of the lines to jump to any of three positions. Subjects could exert force on an immobile lever to move the other line towards the target line. Equal increments of force produced equal displacements of the line. Thus more isometric force was needed to move the line over a larger distance to the target line.

Figure 13.4 defines the major variables of their analysis. The force target is represented by the solid black horizontal line. If the subject performs errorlessly—that is, reaches target without overshoot—the value of the peak force will equal the value of the force target, as in the black curve. Overshoots and undershoots in force are represented by the gray and dashed curves, respectively. Figure 13.5 plots the data of Gordon and Ghez (1987b) in a way that illustrates duration invariance. The horizontal line through the data points shows that force rise time is essentially

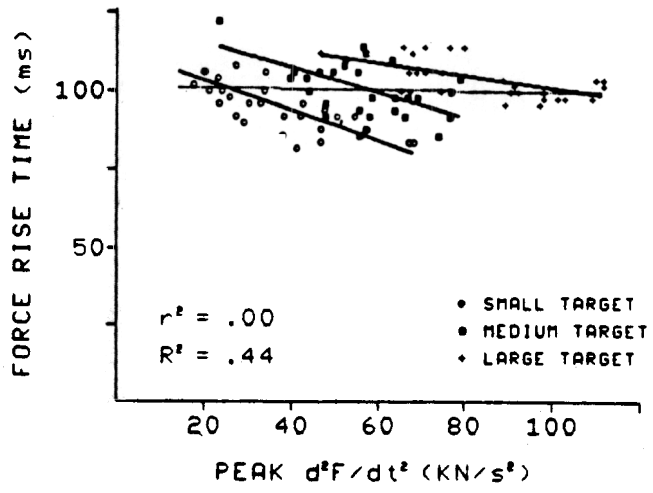

Figure 13.5. Duration invariance across three force target levels. Oblique lines indicate an inverse relation between rise time (duration) and peak acceleration across trials with the same force target level. These trends overlay a direct relation between target level and peak acceleration. Reprinted with permission from Gordon and Ghez (1987b).

independent of peak force acceleration $(\frac{d_2F}{dt_2})$ for all the target distances.

Gordon and Ghez (1987b) separately analysed the data for each of the three target distances, and thereby derived the three oblique lines in Figure 13.5. They interpreted these lines as evidence for an "error correction" process because a negative correlation exists between peak acceleration and the force rise time, or duration. Thus, if the acceleration for a small target distance was too high early in a movement, the trajectory was "corrected" by shortening the rise time. Had this compensation not occurred, the high acceleration could have produced a peak force appropriate for a larger target distance.

Gordon and Ghez (1987b) assumed that trajectories are preplanned and that their peak accelerations are a signature indicating which trajectory has been preplanned. It is from this perspective that they interpreted the compensatory effect shown in Figure 13.5 as an "error correction" process. In contrast, we suggest in Sections 13.13 and 13.21 that this compensatory effect is one of the automatic properties whereby PPC's are gradually updated. We hereby provide an explanation of the compensatory effect that avoids invoking a special mechanism of "error correction" for a movement which does not generate an error in achieving its target. In addition, this explanation provides a unified analysis of the Bizzi *et*

al. (1984) data on isotonic movements and the Gordon and Ghez (1987b) data on isometric contractions.

13.11. Target Switching Experiments: Velocity Amplification, GO Signal, and Fitts' Law

Our explanation of the Freund and Büdingen (1978) and Gordon and Ghez (1987a) data considers how a single GO signal, which initiates and drives all movements to completion, ensures duration invariance when applied to all components of the synergy defined by a TPC. Georgopoulos, Kalaska, and Massey (1981) have collected data which provide further evidence pertinent to the hypothesized interaction of a GO signal with the process which instates a TPC and thereby updates the PPC. In their experiments, monkeys were trained to move a lever from a start position to one of eight target positions radially situated on a planar surface. Then the original target position was switched to a new target position at variable delays after presentation of the first target.

Part of the data confirm the fact that "the aimed motor command is emitted in a continuous, ongoing fashion as a real-time process that can be interrupted at any time by the substitution of the original target by the new one. The effects of this change on the ensuing movement appear promptly, without delays beyond the usual reaction time" (p.725). Figure 13.6 depicts movement paths found during the target switching condition. We explain these data in terms of how instatement of a second TPC can rapidly modify the future updating of the PPC.

In addition, Georgopoulous *et al.* (1981) found a remarkable amplification of peak velocity during the switched component of the movement: "the peak velocity attained on the way to the second target was generally much higher (up to threefold) than that of the control ... these high velocities cannot be accounted for exclusively by a mechanism that adjusts peak velocity to the amplitude of movement ... The cause of this phenomenon is unclear" (pp.732-733). In Section 13.25, we explain this phenomenon in terms of the independent control, or factorization, of the GO mechanism and the TPC-switching mechanism that was described in Section 13.4. In particular, the GO signal builds up continuously in time. When the TPC is switched to a new target, the PPC can be updated much more quickly because the GO signal which drives it is already large. The more rapid updating of the PPC translates into higher velocities.

These target switching data call attention to a more subtle property of how a GO signal energizes PPC updating, indeed a property which has tended to mask the very existence of the GO signal: How can a GO signal which was activated with a previous TPC interact with a later TPC without causing errors in the ability of the PPC to track the later TPC? How does the energizing effect of a GO signal transfer to any TPC? A solution of this problem is suggested in Section 13.18.

The fact that peak velocity is amplified without affecting movement accuracy during target switching implies a violation of Fitt's Law, as Massey, Schwartz, and Georgopoulous (1985) have noted. Our mechanistic analy-

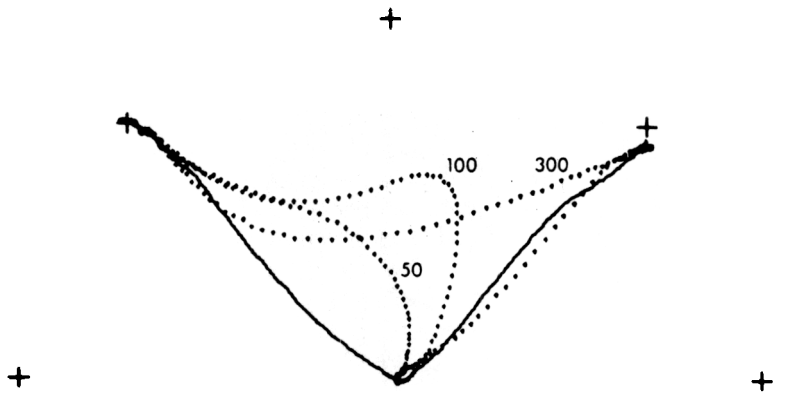

Figure 13.6. Monkeys seamlessly transformed a movement initiated toward the 2 o'clock target into a movement toward the 10 o'clock target when the latter target was substituted 50 or 100 msec. after activation of the 2 o'clock target light. Reprinted with permission from Georgopoulos *et al.* (1981).

sis of synergetic binding via instatement of a TPC and of subsequent PPC updating energized by a previously activated GO signal provides an explanation of this Fitts' Law violation as well as of Fitts' Law itself (Section 13.28).

Our model also suggests an explanation of why the position of maximal curvature and the time of minimal velocity are correlated during two-part arm movements (Abend, Bizzi, and Morasso, 1982; Fetters and Todd, 1987; Viviani and Terzuolo, 1980). This correlation arises in the model if the second TPC is switched on only after the PPC approaches the first TPC. In the Georgopoulous *et al* (1981) experiment, in contrast, the second TPC is switched on due to the second light before the arm reaches the first target. An unanswered question of considerable interest is whether a second GO signal is switched on gradually with the second TPC in the Abend *et al* (1982) paradigm, or whether the reduction in velocity at the turning point is due entirely to nulling of the difference between the PPC and the first TPC while the GO signal maintains an approximately constant value. These alternatives can be tested by measuring the velocities and accelerations subsequent to the position of the turning point.

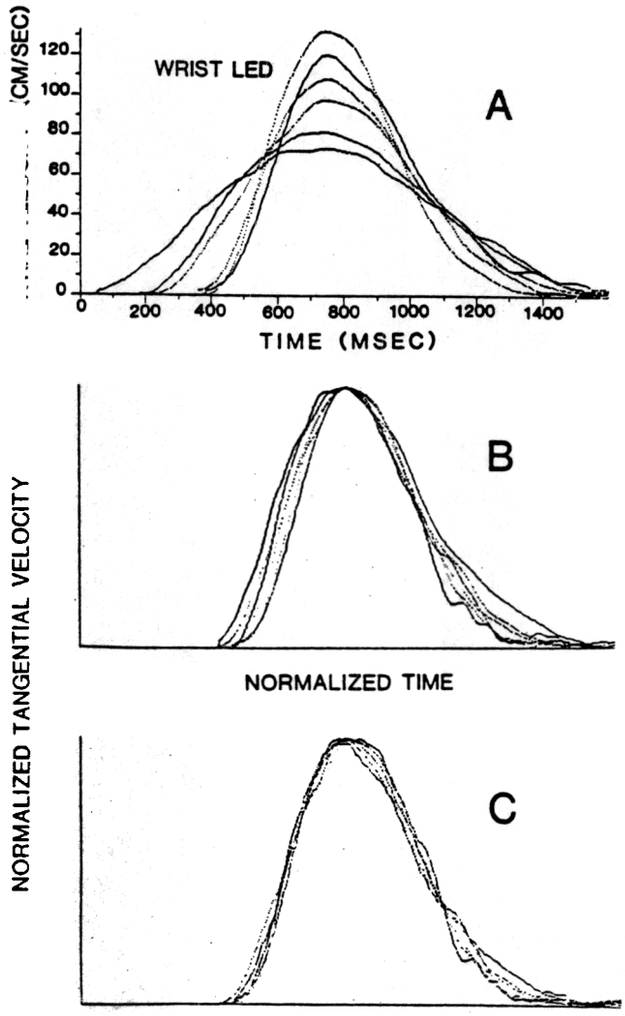

Figure 13.7. Velocity profiles from movements of similar duration are approximately superimposable following velocity and time axis rescaling. Reprinted with permission from Atkeson and Hollerbach (1985).

13.12. Velocity Profile Invariance and Asymmetry

Many investigators have noted that the velocity profiles of simple arm movements are approximately bell-shaped (Abend, Bizzi, and Morasso, 1982; Atkeson and Hollerbach, 1985; Beggs and Howarth, 1972; Georgopoulous, Kalaska, and Massey, 1981; Howarth and Beggs, 1971; Morasso, 1981; Soechting and Lacquaniti, 1981). Moreover the shape of the bell, if rescaled appropriately, is approximately preserved for movements that vary in duration, distance, or peak velocity. Figure 13.7 shows rescaled velocity profiles from the experiment of Atkeson and Hollerbach (1985). These velocity profiles were generated over a fixed distance at several different velocities. Thus both the duration scale and the velocity scale were modified to superimpose the curves shown in Figure 13.7.

On the other hand, Beggs and Howarth (1972) showed that "at high speeds the approach curves of the practised subjects are more symmetrical than at low speeds" (p.451), and Zelaznik, Schmidt, and Gielen (in press) have shown that at very high speeds the direction of asymmetry has actually reversed. Thus the trend documented by Beggs and Howarth continues beyond the range of speeds they sampled. Since velocity profiles associated with slow movements are more asymmetric than those associated with fast movements, they cannot be exactly superimposed. All the velocity profiles shown in Figure 13.7 are taken from slow (1–1.6 sec) movements, and exhibit the sort of more gradual deceleration than acceleration that Beggs and Howarth (1972) reported for such movements.

Asymmetry, its degree, and changes in its direction are of major theoretical importance. For example, the Minimum-Jerk Model of Hogan (1984) predicts symmetric velocity profiles. More generally, superimposability of velocity profiles after time-axis rescaling is a defining characteristic of "generalized motor program" models (Hogan, 1984; Meyer, Smith, and Wright 1982; Schmidt, Zelaznik, and Frank, 1978), which therefore cannot explain how the degree of velocity profile asymmetry varies with overall movement speed. In contrast, our model shows how the gradual updating of the PPC can generate velocity profiles which exhibit the type of speed-dependent asymmetry that is found in the data (Section 13.23).

Both the existence of asymmetry in velocity profiles and the dependence of degree and direction of asymmetry upon movement speed indicate the need for an analysis of the neural dynamics whereby a trajectory unfolds in real-time. In contrast, the Hogan (1984) model's global optimization criterion forces strict superimposability of rescaled velocity profiles because it does not represent a process of temporal unfolding. Beggs and Howarth (1972) suggested that the asymmetry reflects a learned strategy of approaching the target as quickly as possible before making corrective movements near the target. For example, these corrective movements could be made under visual guidance by instating a corrected TPC as the arm approached the target. The approach to such a new TPC would take more time, on the average, than the final approach to the previously tracked TPC, thereby causing greater velocity profile asymmetry. In our simulation results, velocity profiles become more symmetric as movement

speed increases and eventually exhibit a symmetry reversal even in the absence of newly instated TPC's. Thus the greater symmetry of velocity profiles at higher speeds may be due to the combined effects of PPC updating properties as the GO signal is parametrically increased, and to the consequent elimination of corrective TPC's as the target is rapidly approached. In support of this analysis, Jeannerod (1984, p.252) noted that "the low velocity phase is still observed in the absence of visual feedback, and even in the no-vision situation. This finding, however, does not preclude that visual feedback, when present, will be incorporated ... In the present study, movement duration and low-velocity phase duration were found to be increased in the visual feedback situation."

In summary, our explanation of these data shows how a circuit capable of flexibly binding muscle groups into synchronous synergies automatically implies the trends observed in data on velocity profile asymmetry. Thus we suggest an explanation of movement invariants, such as duration invariance and synchrony, using a control circuit which never computes an explicit trajectory and whose outputs exhibit a type of speed-dependent asymmetry which other models have not been able to explain.

13.13. Vector Cells in Motor Cortex

Before quantitatively developing our model, it remains to indicate how the present position command (PPC) is gradually updated until it matches a fixed target position command (TPC). Sections 13.15–13.18 motivate this mechanism through an analysis of the types of information that can be used by a developing system to learn TPC's. The summary here is merely descriptive and is made to link these introductory remarks to supportive neural data.

When a new TPC is switched on, its relationship to the current PPC can be arbitrary. Any realizable pair of positions can be coded by the TPC and the PPC. In order to track the TPC, the PPC needs to change in a *direction* determined by the difference between the TPC and the PPC. In addition, the *amount* of required change is also determined by this difference. An array which measures both the direction and the distance between a pair of arrays TPC and PPC is called a *difference vector*, or DV. At any given time, the DV between the TPC and the PPC—namely, $DV = TPC - PPC$—is computed at a match interface (Figure 13.8).

How does such a DV (difference vector) update the current PPC? Clearly the PPC must be updated in the direction specified by the DV. Hence we assume that the PPC cumulatively adds, or *integrates*, through time all the DV's which arise at the match interface. Due to this arrangement, the PPC gradually approaches the TPC. At a time when the PPC equals the TPC, the DV equals zero; hence, although the PPC may continue to integrate DV's, it will not further change until either the switching on of a new TPC creates a non-zero DV, or the PPC is updated by inflow information during a passive movement (Section 13.30). To summarize these relations, we call our model the Vector-Integration-To-Endpoint (VITE) Model.

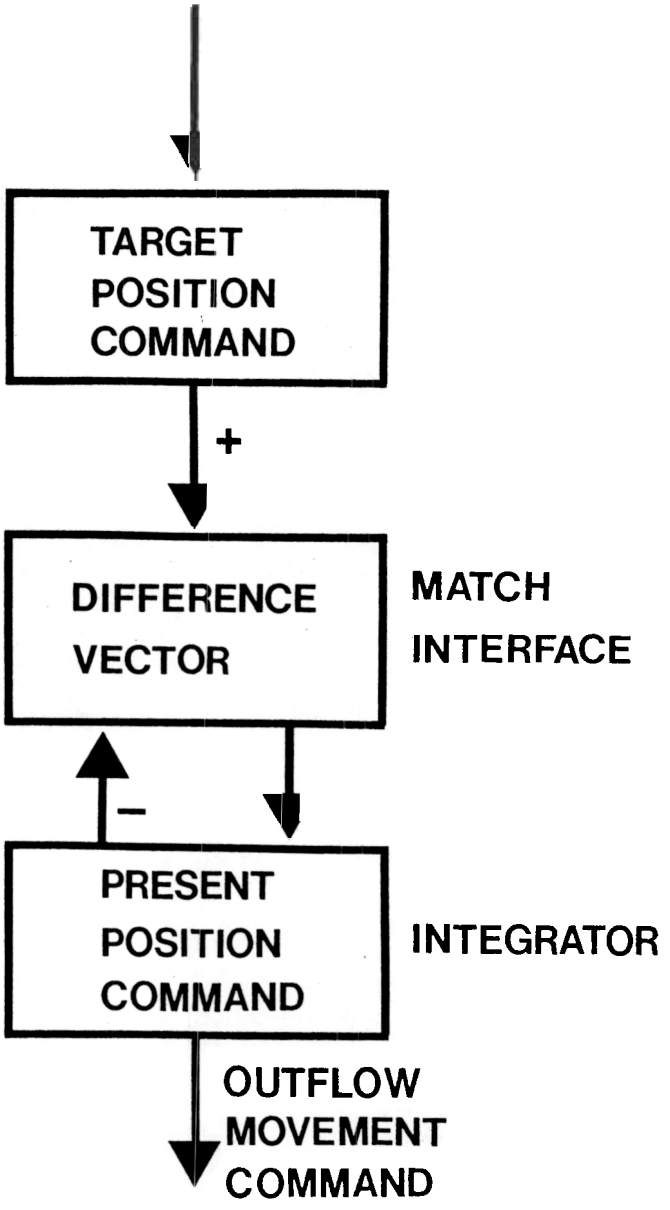

Figure 13.8. A match interface within the motor command channel continuously computes the difference between the target position and present position, and adds the difference to the present position command.

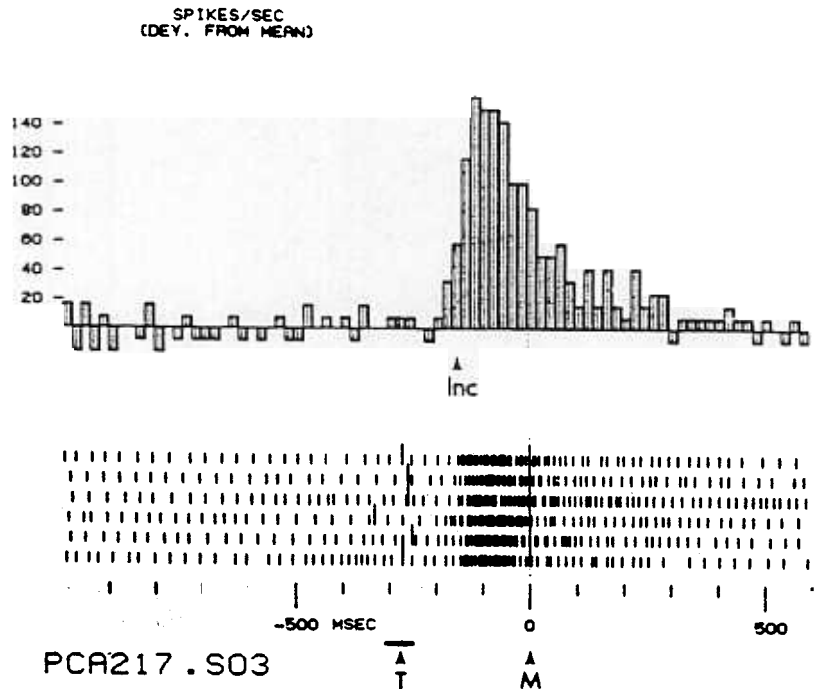

Figure 13.9. Quick buildup and gradual decline of activity in motor-cortical vector cells. Reprinted with permission from Georgopoulos *et al.* (1982).

Georgopoulos and his colleagues (Georgopoulos, Kalaska, Caminiti, and Massey, 1982; Georgopoulos, Kalaska, Crutcher, Caminiti, and Massey, 1984) have found cell populations in the motor cortex whose collective properties mirror those of the vector-computing nodes at the match interface of our model (Figure 13.8). The activity of each such node models the average potential of a population of neural cells with similar receptive field properties. Figure 13.9 shows a histogram of the average number of spikes per unit time recorded from a single such neuron. This temporal behavior closely matches that of a DV cell population in the model (Figure 13.18). The vector cells in motor cortex, just like the DV cell populations in the model, are very broadly tuned to direction (Figure 13.10a); that is,

there exists a broad range of directions in which a given component of the model DV is positive.

Figure 13.11 further explicates these properties. Figure 13.11a clarifies why cells at the DV stage may be called vector cells at all. For simple movements, at increasing times $t_o < t_1 < t_2 < \ldots$, the relative sizes of the activities across the DV populations do not change. Hence these populations code a vector direction, even though their individual absolute activities sweep out an approximately bell-shaped curve through time. Figure 13.11b ilustrates that, as movement direction is parametrically changed, the relative activations of an agonist-antagonist pair of DV populations change systematically in such a way that individual populations may remain active over a broad range of directions, as in Figure 13.10a. Figure 13.11b also schematizes the fact that different agonist muscles may remain active over different ranges of direction, depending upon the movement in question. Although Figure 13.11a schematizes a formal DV, this DV may have many components because it controls many muscle groups. In contrast, the 3-dimensional vector which represents the direction of the arm's movement in Euclidean space has only three components. One of the major outstanding problems in arm movement control is to relate the geometry of the high dimensional muscle space with the geometry of Euclidean space.

Due to the importance of explaining why each DV population is sensitive to a broad range of directions, we further comment on this property below. The PPC outflow channels must control several different muscle groups at each joint, and several different joints in each arm. Because of the opponent organization of the muscles (Figure 13.11b), up to one half of the cellular components composing the DV stage will have positive activities during a given movement.

Each initial positive-valued component $DV_i(0) = TPC_i(0) - PPC_i(0) > 0$ of the difference vector DV corresponds to an expected change in length of one of the many muscle groups whose shortening contributes a motion component to the overall limb movement. If there were only one active agonist-antagonist muscle pair driving the movement, the movement would always tend to follow a preferred direction. Where more than one agonist-antagonist pair guides the movement, however, a muscle can facilitate motion along directions other than its preferred direction. In this case, the net direction of limb motion depends upon the relative sizes $DV_i(0) > 0$ of the cooperating agonists, so that each DV_i population can be active across a broad range of movement directions, as in Figure 13.11b. Since the net movement direction shifts continuously with the relative sizes $DV_i(0)$ of the cooperating agonists, it should be possible to predict the direction of a forthcoming limb movement.

Both of these conclusions have been supported by Georgopoulos, Kalaska, Crutcher, Caminiti, and Massey (1984) and Georgopoulos, Schwartz, and Kettner (1986). Figure 13.10a illustrates that vector cells in motor cortex are, indeed, broadly tuned to direction. Figure 13.10b illustrates that the aggregate activity of a large sample of active vector cells [read,

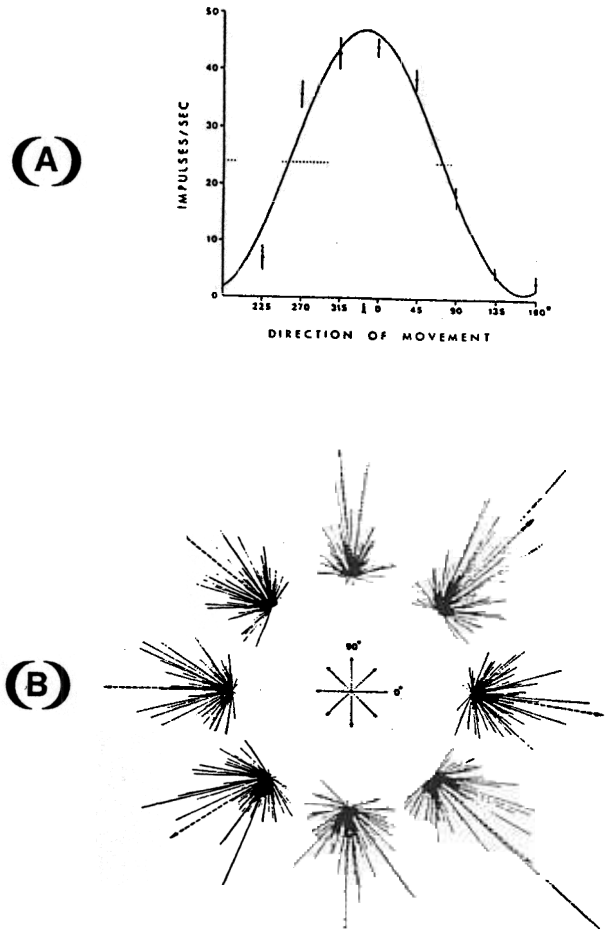

Figure 13.10. (A) Directional tuning curve for a motor-cortical cell exhibiting peak activity during a 0° (center-to-right) arm movement. Dotted line indicates control period discharge rate. Thus this cell is inhibited when movement direction falls outside the 180° hemisphere of movements to which it can contribute a positive motion component. Reprinted with permission from Kalaska *et al.* (1983). (B) Each dotted arrow in the central graphic indicates the direction of a radial (center-out) movement, and points to a representation of the cellular activites observed during that movement. In each plot of cellular activites, the *direction* of each solid black line corresponds to the direction of movement for which a given cell fired maximally, whereas the *length* of each solid black line corresponds to the firing rate of the same cell during the indicated movement. The single dashed line with arrowhead in each plot represents the vector sum of all the neural vectors (solid block lines) generated during the indicated movement. Note the correspondence between the direction of the vector sum (dashed line with arrowhead) and the direction of the actual movement (indicated by the dotted arrow in the central graphic). All cells were related to muscle groups acting at the shoulder, a ball-and-socket joint. Figures reprinted with permission from Georgopoulos *et al.* (1984).

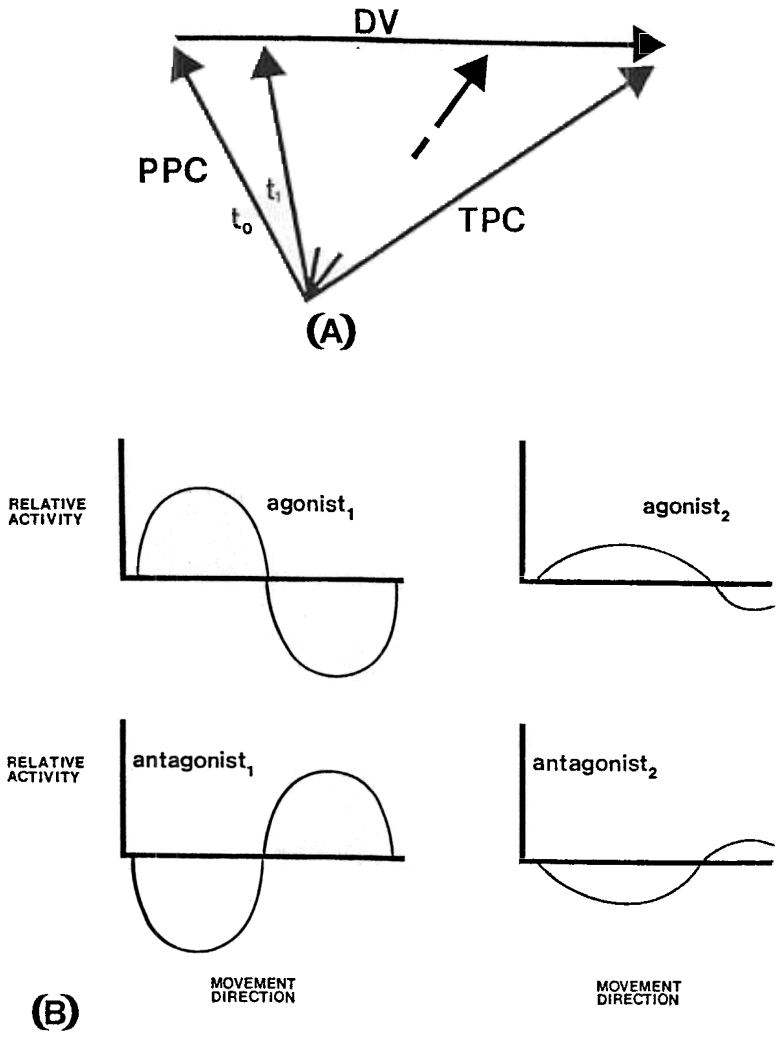

Figure 13.11. (A) As the movement unfolds through times $t_o, t_1, t_2, \ldots$ the present position command (PPC) approaches the target position command (TPC) in such a way that the difference vector (DV) does not change direction as its length approaches zero. (B) Over a full range of movement directions, DV cells associated with opposing muscles (AG_1 *vs.* $ANTAG_1$ or AG_2 *vs.* $ANTAG_2$) show reciprocal patterns of activation and inhibition. The zero-crossings can occur at different points along the direction scale for different opponent pairs (AG_1 - $ANTAG_1$ *vs.* AG_2 - $ANTAG_2$).

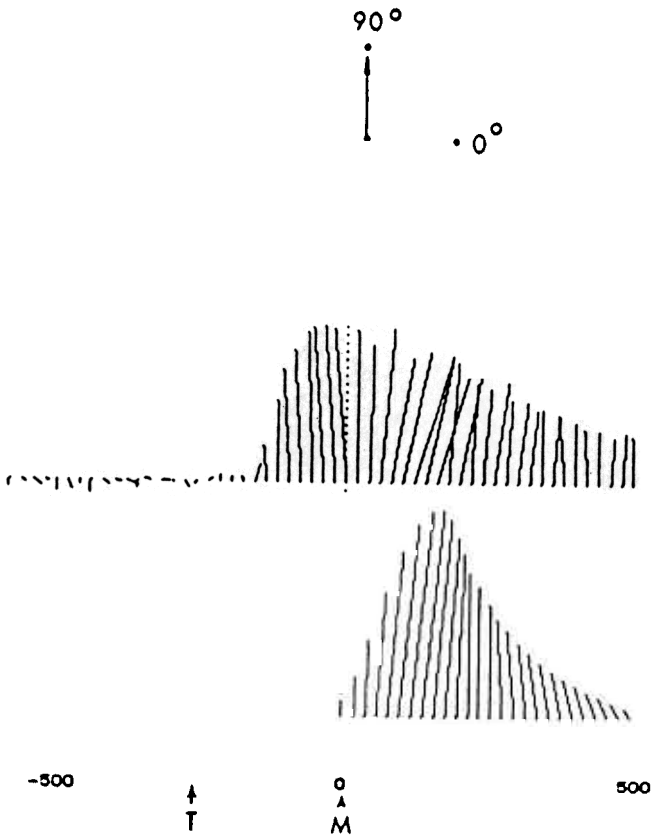

Figure 13.12. (A): A comparison of the population vector of 241 directionally tuned cells (upper figure) with the velocity vector of the hand (lower figure), each measured at 20 msec. intervals during the reaction time and during movement. Note the asymmetry (longer right tail) in both. Reprinted with permission from Georgopoulos *et al.* (1984).

cells from different DV_i populations] can be used to accurately predict the direction of the forthcoming movement.

Figure 13.12 plots data from a vector cell population *in vivo* alongside the velocity profile of the corresponding movement. Note that the asymmetry in the velocity profile is in the same direction as the asymmetry in the vector cell population profile. This correspondence suggests that the velocity asymmetry is related to the neural control circuit, as our model also suggests.

Georgopoulos *et al.* (1984, p.510) also noted that: "No obvious invariance in cell discharge was observed when the final position was the same ... these results show that, at the level of motor cortex, it is the direction

of movement and not its endpoint that is the principle determinant of cell discharge during the initiation and execution of movement. Therefore, if the hypothesis be true that the endpoint of the movement is the controlled spatial variable (Polit and Bizzi, 1979) then the motor cortex seems to be distal to that end-point specifying process." In other words, if one accepts the STE Model, these data suggest that the TPC cells occur closer to the periphery than the DV cells. On the other hand, if one accepts our model, these data imply that the PPC cells occur closer to the periphery than the DV cells, but that the TPC cells occur more central than the DV cells. A combination of anatonomical and physiological experiments can be used to test this prediction. It should also be noted, however, that the STE Model on which the conclusion of Georgopoulos *et al.* (1984) is based is inconsistent with the very existence of vector cells, because the spring-like properties of the muscles themselves, rather than a neural computation of vectors, determines the direction and length of movement in the STE Model.

Several further properties of cells in precentral motor cortex, documented by Evarts and Tanji (1974; Tanji and Evarts, 1976), lend support to identifying them with the vector cells in our model. In their experiments, monkeys were trained to either push or pull a lever. During each trial (schematized in Figure 13.13a) animals first held the lever in a medial position for 2-4 sec. Then either a green or a red *priming* signal was illuminated. If green, the forthcoming movement required for reward was a push; if red, a pull. Finally, .6–1.2 seconds after the priming signal, the *release* signal occurred. This release signal took the form of an externally imposed push or pull on the lever held by the monkey. It both cued movement onset and perturbed the position of the lever so as to increase or decrease its initial distance from target.

Figure 13.13b summarizes operating characteristics of two cells. The first cell increased its activity after a "push" priming signal, but was inhibited by a "pull" priming signal; the second cell showed the opposite response. From these data alone, it would not be clear whether these cells' activities code DV's or TPC's. However, their further characteristics confirm their status as DV cells. The second bracket for each cell in Figure 13.13b indicates that their activities decline as movement proceeds in their preferred direction. This decline rules out the TPC interpretation. In the model, it occurs because the movement progressively cancels the difference with which DV cell activity is correlated.

The third bracket for each cell indicates that the initial position perturbations also have the effect they must have if the DV interpretation is correct: perturbations that make the starting point closer to target subtract from activity levels, whereas contrary perturbations add to activity levels. This occurs automatically in the model because PPC's, and thus the corresponding DV's, are updated by sensory feedback during passive movements (Section 13.30).

Though the foregoing considerations argue strongly for the existence of DV cells in precentral motor cortex, it might be argued that the DV's

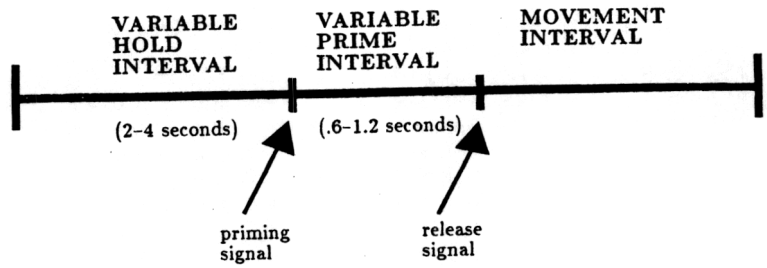

(A)

CELL 1 OPERATING CHARACTERISTICS

⇑ priming signal	produced	↑ activity
⇓ priming signal	produced	↓ activity
⇑ movement	produced	↓ activity
⇑ prime + ⇓ perturbation	produced	greater ↑ activity
⇑ prime + ⇑ perturbation	produced	less ↑ activity

CELL 2 OPERATING CHARACTERISTICS

⇓ priming signal	produced	↑ activity
⇑ priming signal	produced	↓ activity
⇓ movement	produced	activity
⇓ prime + ⇑ perturbation	produced	greater ↑ activity
⇓ prime + ⇓ perturbation	produced	less ↑ activity

(B)

Figure 13.13. (A): The time course of each trial in the push-or-pull task used by Evarts and Tanji (1974). (B): Operating characteristics of two motor-cortical cells. Solid arrows indicate increases (upward arrow) or decreases (downward arrow) in cell discharge rates. Hollow arrows indicate a push-(upward arrow) or pull-(downward arrow) related event: either the push/pull priming signal, a push/pull movement, or the push/pull perturbation that also served as the release signal.

could be measuring force rather than positional values. Indeed, Evarts interpreted his early experimental data (Evarts, 1968) as suggestive of force coding. However, the data of Schmidt, Jost and Davis (1975) appear to rule out this alternative interpretation. After varying position and force independently, they concluded that "motor cortex cell firing patterns appear to be unrelated to the large values of rate of change of force seen in this experiment" (p.213).

The data summarized in Sections 13.7–13.13 weigh heavily against the STE Model and models based upon optimization principles. So too do the formal shortcomings of these models noted in Sections 13.7 and 13.12. We now show that the Vector-Integration-to-Endpoint (VITE) Model overcomes these formal shortcomings and provides a parsimonious quantitative explanation of all the behavioral and neural data summarized above and in the subsequent sections.

13.14. Learning Constraints Mold Arm Control Circuits

Rejecting the Spring-To-Endpoint (STE) Model does not entail rejecting all dependence upon endpoint commands. An analysis of sensory-motor learning during eye-hand coordination enables us to identify processes which supplement endpoint, or target position, commands to overcome the shortcomings of the STE Model (Grossberg, 1978a). The central role of learning constraints in the design of sensory-motor systems has elsewhere been developed for the case of the saccadic eye movement system (Grossberg and Kuperstein, 1986).

We focus our discussion of learning within the arm movement system upon the basic problem of how, when an observer looks at an object, the observer's hand knows where to move in order to touch the object. We discuss this issue from the perspective of eye-hand coordination in a mammal, but the issues that are raised, as well as the conclusions that are drawn, generalize to many other species and sensory-motor systems. Why learning processes are needed to solve this problem is illustrated by the following example.

The movement command which guides the hand to a visual target at a fixed position relative to the body is not invariant under growth. If a young arm, with relatively short limb segments, and an old arm with relatively long limb segments, react to the same command—that is, assume equal angles at analogous joints—then the tips of the two arm's fingers will be at different loci with respect to the body frame. In short, any animal that grows over an extended period will need to adaptively modify movement commands even if its only ambition is to perform the same act earlier and later in its life cycle. Put the other way, that animals do remain able to reach desired targets throughout periods of limb growth implies plasticity in their sensory-motor commands. Because such growth is slow relative to the rate of learning, failures of sensory-motor coordination are rarely noticeable. In humans, exceptions occur during the first few months of life, prior to experiential tuning of the infant's initially coarse sensory-motor mapping (Fetters and Todd, 1987; von Hofsten, 1979, 1982).

13.15. Comparing Target Position with Present Position to Gate Intermodality Learning

Thus, as the arm grows, the motor commands which move it to a fixed position in space with respect to the body must also change through learning. Many arm movements are activated in response to visually seen objects that the individual wishes to grasp. We therefore formulate this learning process as follows: How is a transformation learned and adaptively modified between the parameters of the eye-head system and the hand-arm system so that an observer can touch a visually fixated object?

Following Piaget's (1963) analysis of *circular reactions*, let us imagine that an infant's hand makes a series of unconditional movements, which the infant's eyes unconditionally follow. As the hand occupies a variety of positions that the eye fixates, a transformation is learned from the parameters of the hand-arm system to the parameters of the eye-head system. A reverse transformation is also learned from parameters of the eye-head system to parameters of the hand-arm system. This reverse transformation enables an observer to intentionally move its hand to a visually fixated position.

How do these two sensory-motor systems know what parameters are the correct ones to map upon each other? This question raises the fundamental problem that many neural signals, although large, are unsuitable for being incorporated into behavioral maps and commands. They are "functional noise" to the motor learning process. The learning process needs to be actively modulated, or gated, against learning during inappropriate circumstances.

In the present instance, not all positions that the eye-head system or the hand-arm system assume are the correct positions to associate through learning. For example, suppose that the hand briefly remains at a given position and that the eye moves to foveate the hand. An infinite number of positions are assumed by the eye as it moves to foveate the hand. Only the final, intended, or expected position of the eye-head system is a correct position to associate with the position of the hand-arm system.

Learning of an intermodal motor map must thus be prevented except when the eye-head system and the hand-arm system are near their intended positions. Otherwise, all possible positions of the two systems could be associated with each other, which would lead to behaviorally chaotic consequences. Several important conclusions follow from this observation (Grossberg, 1978a; Grossberg and Kuperstein, 1986).

(1) All such adaptive sensory-motor systems compute a representation of target position (also called expected position, or intended position). Thus the importance of endpoint computations is confirmed. This representation is the TPC (target position command). In addition:

(2) All such adaptive sensory-motor systems also compute a representation of present position. This representation is the PPC (present position command).

(3) During movement, target position is matched against present po-

sition. Intermodal map learning is prevented except when target position approximately matches present position (Figure 13.14). A *gating*, or modulator, signal is thus controlled by the network at which target position is matched with present position. This gating signal enables learning to occur when a good match occurs and prevents learning from occurring when a bad match occurs. This matching process takes place at the match interface that was described in Section 13.13. The DV (difference vector) controls the gating signal.

(4) In order to compare target positions with present positions, both types of data must be computed in the same coordinate system. Present eye position is computed with respect to head coordinates. Thus there is an evolutionary pressure to encode target position in head coordinates.

13.16. Trajectory Formation using DV's: Automatic Compensation for Present Position

The above discussion of how *intermodality* sensory-motor transformations are learned also sheds light upon how *intramodality* movement trajectories are formed. Intermodality transformations associate TPC's because only such transformations can avoid the multiple confusions that could arise through associating arbitrary positions along a movement trajectory. TPC's are not, however, sufficient to generate intramodality movement trajectories. In response to the same TPC, an eye, arm, or leg must move different distances and directions depending upon its present position when the target position is registered.

PPC's can be used to convert a single TPC into many different movement trajectories. Computation of the difference between target position and present position at the match interface in Figure 13.8 generates a difference vector, or DV, that can be used to automatically compensate for present position. Such automatic compensation accomplishes a tremendous reduction in the memory load that is placed upon an adaptive sensory-motor system. Instead of having to learn whole movement trajectories, the system only has to learn intermodality maps between TPC's. As shall be shown below, the DV's which are computed from target positions and present positions at the match interface can be used to automatically and continuously update the PPC movement commands from which the trajectory is formed. In summary, consideration of the types of information that can be used to learn intermodality commands during motor development leads to general conclusions about the quantities from which intramodality movement trajectories are formed, and thus about the way in which other neural systems, such as sensory, cognitive, and motivational systems, can influence the planning of such trajectories.

Computation of TPC's, PPC's, and DV's is a qualitatively different approach to generating a trajectory than are traditional computations based upon a Newtonian analysis of movement kinematics. In a Newtonian analysis, every position within the trajectory is assumed to be explicitly controlled (Atkeson and Hollerbach, 1985; Brody and Paul, 1984; Hogan, 1984; Hollerbach, 1984). Such computations lead to a combinatorial ex-

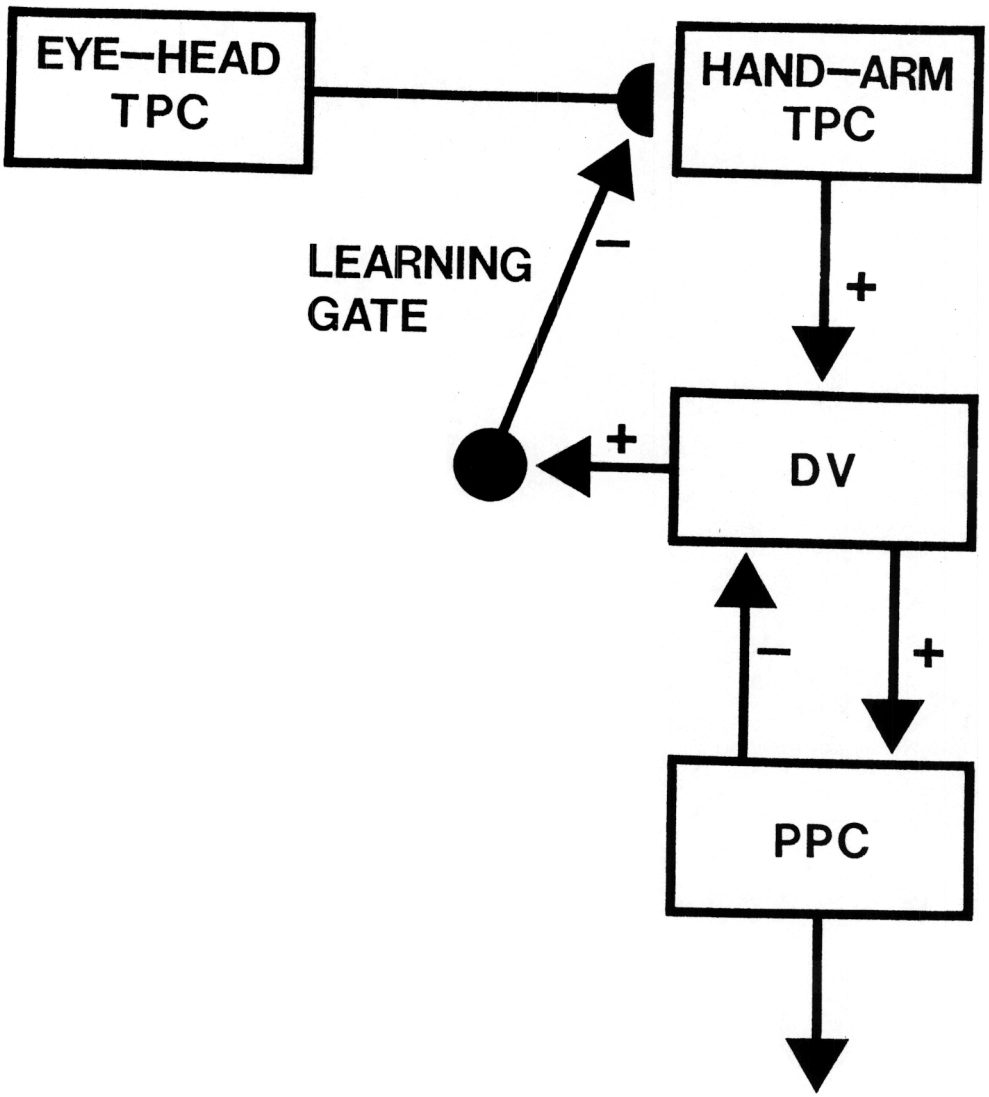

Figure 13.14. Learning in sensory-motor pathways is gated by a DV process which matches TPC with PPC to prevent incorrect associations from forming between eye-head TPC's and hand-arm TPC's.

plosion which is hard to reconcile with the rapidity of biological movement generation in real-time. In a vector computation, the entire trajectory is never explicitly planned. Instead, a TPC is computed which determines where the movement expects, or intends, to terminate. The subtraction of the PPC is an automatic process which compensates for the variability of the starting position. The DV which is hereby computed can be used to generate an accurate movement without ever explicitly computing a planned sequence of trajectory positions for the whole movement. In arm movements, a continuous comparison is made between a fixed TPC and all the PPC's that are computed during the movement. All of these compensations for changes in present position are automatically registered, and therefore place no further burden upon the computation of planned movement parameters. In addition, such automatic compensations for present position spontaneously generate the major invariants of arm movements that have been discovered to date (Sections 13.22–13.29). Thus the general problem of how DV's are computed is a central one for the understanding of trajectory formation in several movement systems.

13.17. Matching and Vector Integration during Trajectory Formation

We now specify in greater detail a model of how TPC's, PPC's, and DV's interact with each other through time to synthesize a movement trajectory. Each PPC generates a pattern of outflow movement signals to arm system muscles (Figure 13.8). Each such outflow pattern acts to move the arm system towards the present position which it encodes. Thus, were only a single PPC to be activated, the arm system would come to rest at a single physical position. A complete movement trajectory can be generated in the form of a temporal succession of PPC's. Such a movement trajectory can be generated in response to a single TPC that remains active throughout the movement. Although a TPC explicitly encodes only the endpoint of the movement, the process whereby present positions are automatically and continuously updated possesses properties that are much more powerful than those of an STE Model.

This process of continuous updating proceeds as follows. At every moment, a DV is computed from the fixed TPC and the PPC (Figure 13.8). This DV encodes the difference between the TPC and the PPC. In particular, the DV is computed by subtracting the PPC from the TPC at the match interface.

Because a DV computes the difference between the TPC and the PPC, the PPC equals the TPC only when all components of the DV equal zero. Thus, if the arm system's commands are calibrated so that the arm attains the physical position in space that is coded by its PPC, then the arm system will approach the desired target position in space as the DV's computed during its trajectory approach zero. This is accomplished as follows.

At each time, the DV computes the direction and amplitude which must still be moved to match the PPC with the TPC. Thus the DV com-

putes an error signal of a very special kind. These error signals are used to continuously update the PPC in such a way that the changing PPC approaches the fixed TPC by progressively reducing the vector error to zero. In particular, the match interface at which DV's are computed sends excitatory signals to the stage where PPC's are computed. This stage integrates, or adds up, these vector signals through time. The PPC is thus a cumulative record of all past DV's, and each DV brings the PPC a little closer to the target position command.

In so doing, the DV is itself updated due to negative feedback from the new PPC to the match interface (Figure 13.8). This process of updating present positions through vector integration and negative feedback continues continuously until the PPC equals the TPC. Several important conclusions follow from this analysis of the trajectory formation process.

Two processes within the arm control system do double duty: A PPC generates feedforward, or outflow, movement signals *and* negative feedback signals which are used to compute a DV. A DV is used to update intramodality trajectory information *and* to gate intermodality learning of associative transformations between TPC's. Thus the match interface continuously updates the PPC when the arm is moving *and* disinhibits the intermodality map learning process when the arm comes to rest.

Within the circuit depicted in Figure 13.8, "position" and "direction" information are separately coded. Positional information is coded within the PPC and directional information is coded by the DV at the match interface. On the other hand, the computations which give rise to positional and directional information are not independent, since DV's are integrated to compute PPC's, and PPC's are subtracted from TPC's to compute DV's.

In Figure 13.8, the PPC is computed using outflow information, but not inflow information. This property emphasizes the need to mechanize concepts about how present position is computed. Using an outflow-based PPC clarifies how targets can be reached when sources of inflow information are eliminated (Polit and Bizzi, 1978) without being forced into the erroneous conclusion that no information about present position is needed to form a trajectory. In addition, although the PPC integrates outflow DV signals during active movements, inflow signals are used to update the PPC during passive movements (Section 13.30), thereby clarifying the data of Polit and Bizzi (1978) concerning failure of monkeys to compensate for passive shifts of their initial upper arm position in the deafferented state. The PPC feedback shown in Figure 13.8 is an "efference copy" of a "premotor" command (von Holst and Mittelsteadt, 1950). The VITE model's use of efferent feedback distinguishes it from an alternative class of models, which propose that present position information is derived from afferent feedback from sensory receptors in the limb. In particular, the far reaching consequences of its use of efferent, as opposed to afferent, feedback make the VITE model fundamentally different from the classical closed-loop servo recommended by Adams (1971, 1977) as a model of human motor performance. Further differences are introduced by the VITE

model's use of the time-varying multiplicative GO signal introduced in Section 13.11 and elaborated below.

13.18. Intentionality and the GO Signal: Motor Priming without Movement

The circuit depicted in Figure 13.8 embodies the concept of intention, or expectation, through its computation of a TPC. The complete movement circuit embodies intentionality in yet another sense, which leads to a circuit capable of variable speed control. The need for such an additional process can also be motivated through a consideration of eye-hand coordination (Grossberg, 1978a, 1982a).

When a human looks at a nearby object, several movement options for touching the object are available. The object could be grasped with the left hand or the right hand. The object could even be touched with one's nose or one's toes! We assume that the eye-head system can simultaneously activate TPC's in several motor systems via the intermodality associative transformations that are learned to these systems. An additional "act of will," or GO signal, is required to convert one or more of these TPC's into overt movement trajectories within only the selected motor systems.

There is only one way to implement such a GO signal within the circuit depicted in Figure 13.8. This implementation is described in Figure 13.15. The GO signal must act at a stage intermediate between the stages which compute DV's and PPC's: The GO signal must act after the match interface so that it does not disrupt the process whereby DV's become zero as PPC's approach the TPC. The GO signal must act before the stage which computes PPC's so that changes in the GO signal cannot cause further movement after the PPC matches the TPC. Thus, although the GO signal changes the outputs from the match interface before they reach the present position stage, the very existence of such processing stages for continuous formation of a trajectory enables the GO signal to act without destroying the accuracy of the trajectory.

The detailed computational properties of the GO signal are derived from two further constraints. First, the absence of a GO signal must prevent the movement from occurring. This constraint suggests that the GO signal multiplies, or *shunts*, each output pathway from the match interface. A zero GO signal multiplies every output to zero, and hence prevents the PPC from being updated. Second, the GO signal must not change the direction of movement that is encoded by a DV. The direction of movement is encoded by the *relative* sizes of all the output signals generated by the vector. This constraint reaffirms that the GO signal *multiplies* vector outputs. It also implies that the GO signal is *nonspecific*: The *same* GO signal multiplies each output signal from the matching interface so as not to change the direction encoded by the vector.

In summary, the GO signal takes a particularly simple form. When it equals zero, the present position signal is not updated. Hence no overt movement is generated. On the other hand, a zero GO signal does not prevent a TPC from being activated, or a DV from being computed. Thus

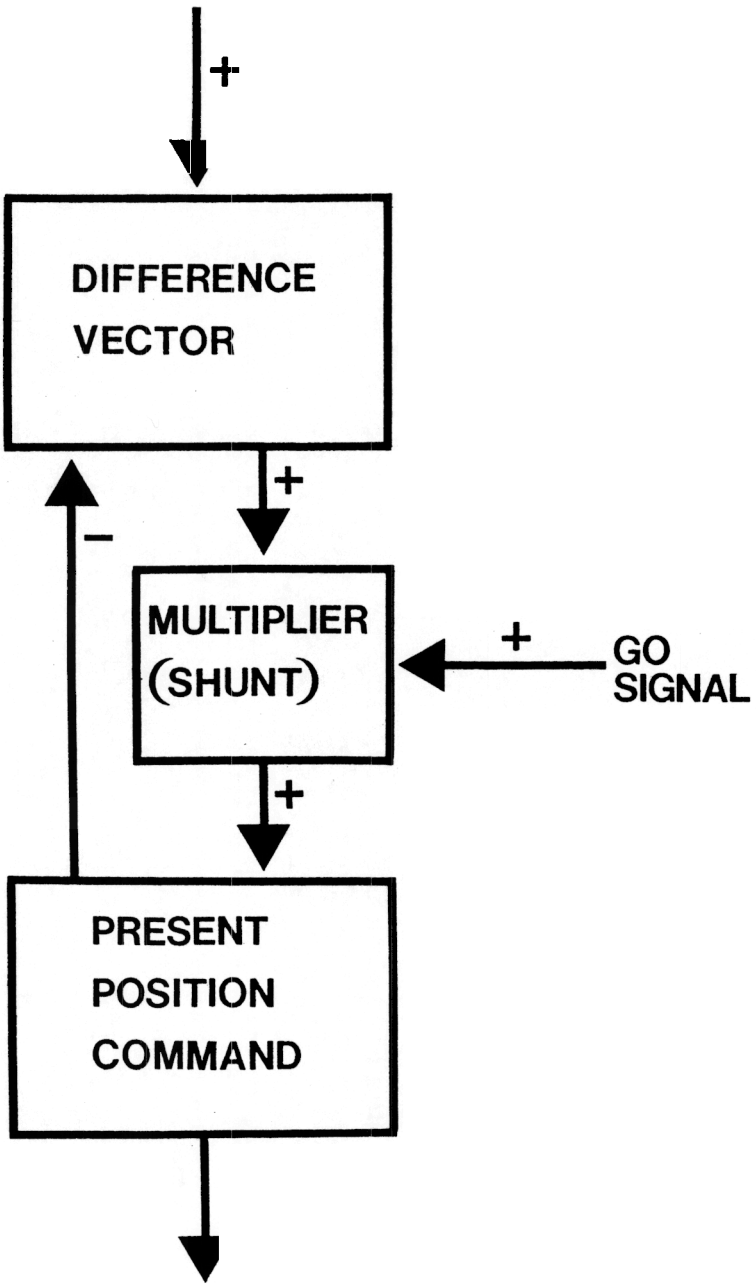

Figure 13.15. A GO signal gates execution of a primed movement vector and regulates the rate at which the movement vector updates the present position command.

a motor system can become ready, or primed, for movement before its GO signal turns on. When the GO signal does turn on, the movement can be rapidly initiated. The size of the GO signal regulates overall movement speed. Larger GO signals cause faster movements, other things being equal, by speeding up the process whereby directional information from the match interface is integrated into new PPC's. In models of cognitive processing, the functional analog of the GO signal is an attentional gain control signal (Carpenter and Grossberg, 1987a, 1988a; Grossberg, 1987b, 1987c; Grossberg and Stone, 1986a).

Georgopoulos, Schwartz, and Kettner (1986) have reported data consistent with this scheme. In their experiment, a monkey is trained to withhold movement for 0.5 to 3 seconds until a lighted target dims. They reported that cells with properties akin to DV cells computed a direction congruent with that of the upcoming movement during the waiting period. These data support the prediction that the neural stage where the GO signal is registered lies between the DV stage and the PPC stage.

13.19. Synchrony, Variable Speed Control, and Fast Freeze

The circuit in Figure 13.15 is now easily seen to possess qualitative properties of synchronous synergetic movement, variable speed control, and fast freeze-and-abort. We apply the circuit properties that each muscle synergist's motor command is updated at a rate that is proportional both to the synergist's distance from its target position and to a variable-magnitude GO signal, which is broadcast to all members of the synergy to initiate and sustain the parallel updating process.

To fix ideas, consider a simple numerical example. Suppose that, prior to movement initiation, muscle synergist A is 4 distance units from its target position and muscle synergist B is 2 distance units from its target position. In that case, if the mean rates at which PPC's are updated for the two synergists are in the same proportion as the distance (i.e., 2:1), then the updating of synergist A will take $4/2$ time units while the updating of synergist B will take $2/1$ time units. Thus both processes will consume approximately 2 time units. Although the PPC updating process occurs at different rates for different synergists, it consumes equal times for all synergists. The result is a synchronous movement despite large rate variations among the component motions.

Changing the magnitude of the GO signal governs variable speed control. Because both of the updating rates in the example (2 and 1) are multiplied by the same GO signal, the component motions will remain synchronous, though of shorter or longer duration, depending on whether the GO signal multiplier is made larger or smaller, respectively. In general, the GO signal's magnitude varies inversely with duration and directly with speed. Finally, if the value of the GO signal remains at zero, no updating and no motion will occur. Thus very rapid freezing can be achieved by completely inhibiting the GO signal at any point in the trajectory. The fact that target position may be very different from present position when the GO signal is withdrawn does not interfere with freezing, as it would

using a STE Model, because the arm position closely tracks the PPC, which stops changing as soon as the signal shuts off.

Grossberg (1978a, Section 54; reprinted in Grossberg, 1982a) suggested an alternative scheme whereby actively moving muscles could be opposed by properly scaled antagonist co-contractions in response to a sudden unexpected event. In this scheme, agonist-antagonist motor commands are organized as gated dipole opponent processes and the unexpected event triggers a burst of nonspecific arousal to all the command sources. Each gated dipole opponent process reacts to such a nonspecific arousal burst by causing an antagonistic rebound whose size is scaled to that of the dipole's prior on-response. The rate of antagonist contraction generated by such a scheme is thus matched to the size of the just-previous rate of agonist contraction. Both types of mechanism—inhibition of GO signal and onset of arousal burst to opponent motor controls—are worthy of further neurophysiological testing. Another role for the opponent organization of motor commands is summarized in the next section.

13.20. Opponent Processing of Movement Commands

Mammalian motor systems are organized into pairs of agonist and antagonist muscles. We now note a new functional role for such an opponent organization: An opponent organization is needed to convert DV's into PPC's which can eventually match an arbitrary TPC. Figure 13.16 depicts how opponent organization is joined to the system's other processing constraints.

The need for opponent signals can be seen from the following examples. If a target position signal is larger than the corresponding present position signal, then a positive output signal is generated by the corresponding component of the DV. Such positive output signals increase the present position signal until it matches the target position signal. Increasing the present position signal causes the target muscle group to contract. The opponent muscle group must also simultaneously relax. Inhibitory signals to the present position node of the opponent muscle instate this latter property. When these inhibitory signals are integrated by the present position node of the opponent muscle, the output signal to the opponent muscle decreases, thereby relaxing the muscle.

The need for opponent processing can also be seen by considering the case in which the target position signal is smaller than the present position signal. Then the corresponding component of the DV is negative. Since only nonnegative activities can generate output signals, no output signal is generated by this component of the DV to its corresponding present position node. How, then, is this present position signal decreased until it matches the target position signal? The answer is now obvious, since we have just considered the same problem from a slightly different perspective: If a negative vector component corresponds to an antagonist muscle group, a positive vector component corresponds to its opponent agonist muscle group. This positive vector component generates inhibitory signals to the present position command of the antagonist muscle, thereby

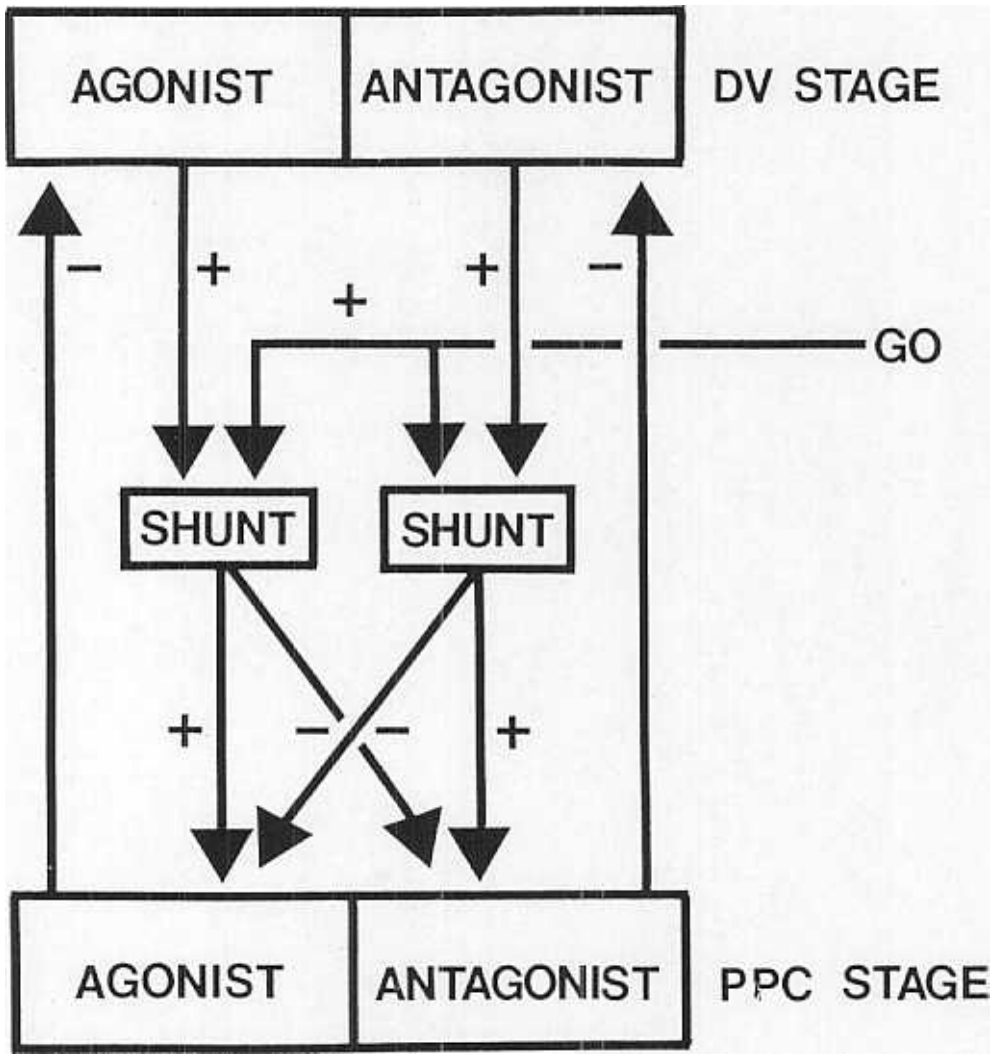

Figure 13.16. Opponent interactions among channels controlling agonists and their antagonists enable coordinated, automatic updating of their present position commands (PPCs). DV = difference vector.

relaxing the antagonist muscle until its PPC equals its TPC.

13.21. System Equations

A quantitative analysis of movement invariants requires the development of a rigorous real-time mathematical model of the constraints summarized in the preceding sections. Qualitative algebraic analysis is insufficient because the trajectory is an emergent property of a nonlinear integration and feedback process under variable gain control. Our model defines the simplest system that is consistent with these constraints. To fix ideas, we explicitly study how the TPC to an agonist muscle group generates a trajectory of PPC signals to that muscle group. Generalizations to synergetic movement of multiple agonist-antagonist muscle groups follow directly from this analysis. Figure 13.17 locates the mathematical variables that are defined below. The network depicted in Figure 13.17 obeys the following system of differential equations:

$$\frac{dV}{dt} = \alpha(-V + T - P) \tag{13.2}$$

and

$$\frac{dP}{dt} = G[V]^+. \tag{13.3}$$

In (13.2) and (13.3), $T(t)$ is a target position input, $V(t)$ is the activity of the agonist's DV population, $P(t)$ is the activity of the agonist's PPC population, $G(t)$ is the GO signal, $\frac{dV}{dt}$ is the rate of change of V, and $\frac{dP}{dt}$ is the rate of change of P.

Equation (13.2) says that the activity $V(t)$ averages the difference of the input signals $T(t)$ and $P(t)$ at a rate α through time. The TPC input $T(t)$ excites $V(t)$, whereas the PPC input $P(t)$ inhibits $V(t)$ as part of the negative feedback loop between $V(t)$ and $P(t)$.

Equation (13.3) says that $P(t)$ cumulatively adds, or integrates, the product $G[V]^+$, where

$$[V]^+ = \begin{cases} V & \text{if } V > 0 \\ 0 & \text{if } V \leq 0. \end{cases} \tag{13.4}$$

In other words, the DV population elicits an output signal $[V]^+$ to the PPC population only if the activity V exceeds the output threshold 0. The output signal is a linear function of V at suprathreshold values. The output signal $[V]^+$ is multiplied, or gated, by the GO signal $G(t)$ on its way to the PPC stage. The activity $P(t)$ at the PPC stage integrates the gated signal through time.

In particular, $G(t) = 0$ implies $\frac{dP}{dt}(t) = 0$. In other words, if the GO signal is shut off within a given time interval, the $P(t)$ is constant throughout that time interval. Fast-freeze can hereby be rapidly obtained

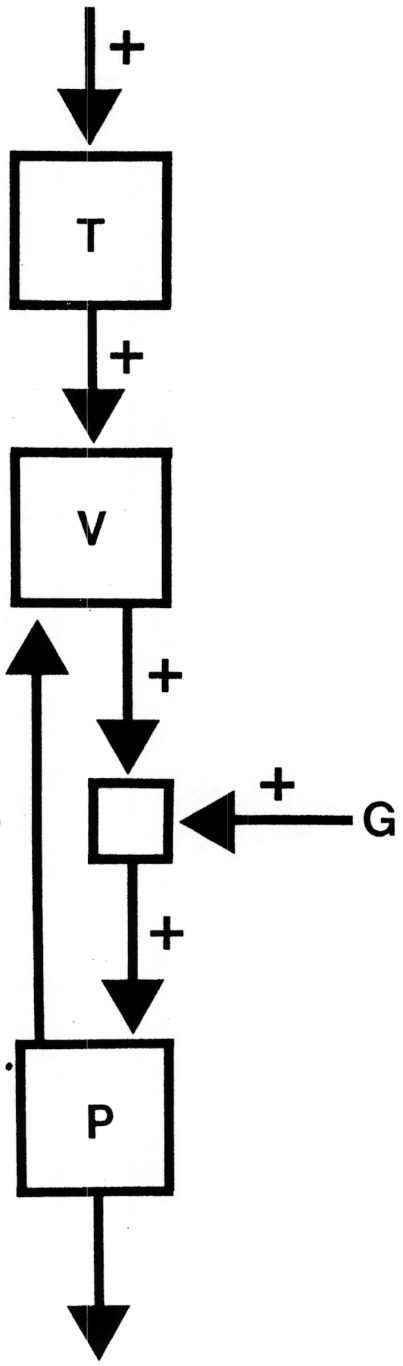

Figure 13.17. Network variables employed in computer simulations. See text equations (13.2) and (13.3).

by simply switching $G(t)$ quickly to zero no matter how far $P(t)$ may be from $T(t)$ at that time. In addition, this circuit generates compensatory, or "error correcting," trajectories, as described in Section 13.10. For example, suppose that the GO signal starts out larger than usual or that there is a slight delay in instatement of the TPC relative to onset of the GO signal. In either case, $P(t)$ can initially increase faster than usual. As a result, $T - P(t)$ can rapidly become smaller than usual. Consequently, updating of $P(t)$ terminates earlier than usual.

This compensatory process illustrates two critical features of the VITE Model: (1) Trajectories are not pre-formed. (2) Because the GO signal feeds in between the DV stage and the PPC stage and because the DV is continuously inhibited by feedback from the PPC stage, accuracy is largely insulated from random variations in the size or onset time of the GO signal, variations in the onset time of the TPC, or momentary perturbations of the PPC due to internal noise or inflow signals.

The system of equations (13.2)–(13.4) is explicitly solved for a particular choice of GO signal in Appendix 1. In Sections 13.22–13.29, we display the results of computer simulations which demonstrate that this simple model provides a quantitative explanation of all the data thus far summarized. In most of these simulations, we write the GO signal in the form

$$G(t) = G_0 g(t). \tag{13.5}$$

Constant G_0 is called the GO *amplitude* and function $g(t)$ is called the GO *onset function*. The GO amplitude parameterizes how large the GO signal can become. The GO onset function describes the transient build-up of the GO signal after it is switched on. In our simulations, we systematically studied the influence of choosing different GO amplitudes G_0 and onset functions from the family

$$g(t) = \begin{cases} \frac{t_n}{\beta_n + \gamma t_n} & \text{if } t \geq 0 \\ 0 & \text{if } t < 0. \end{cases} \tag{13.6}$$

In (13.6), we chose β and γ equal to 1 or 0. If $\beta = 0$ and $\gamma = 1$, then $g(t)$ is a step function which switches from 0 to 1 at time $t = 0$. If $\beta = 1$ and $\gamma = 1$, then $g(t)$ is a slower-than-linear function of time if $n = 1$ and a sigmoid, or S-shaped, function of time if $n > 1$. In both of these cases, function $g(t)$ increases from $g(0) = 0$ to a maximum of 1, and attains the value $\frac{1}{2}$ at time $t = \beta$. If $\beta = 1$ and $\gamma = 0$, then $g(t)$ is a linear function of time if $n = 1$ and a faster-than-linear function of time if $n > 1$. We will demonstrate below that an onset function which is a faster-than-linear or sigmoid function of time generates a PPC profile through time that is in quantitative accord with data about the arm's velocity profile through time. On the other hand, if muscle and arm properties attenuate the increase in velocity at the beginning of a movement, then linear or even slower-than-linear onset functions could also quantitatively fit the data. Direct physiological measurements of the GO signal and PPC updating processes would enable a more definitive selection of the onset function to be made.

13.22. Computer Simulation of Movement Synchrony and Duration Invariance

In simulations of synchronous contraction, the same GO signal $G(t)$ is switched on at time $t = 0$ across all VITE circuit channels. We consider only agonist channels whose muscles contract to perform the synergy. Antagonist channels are controlled by opponent signals as described in Section 13.20. We assume that all agonist channels start out at equilibrium before their TPC's are switched to new, sustained target values at time $t = 0$. In all agonist muscles, $T(0) > P(0)$. Consequently, $V(t)$ in (13.2) increases, thereby increasing $P(t)$ in (13.3) and causing the target muscle to contract. Different muscles may be commanded to contract by different amounts. Then the size of $T(0) - P(0)$ will differ across the VITE channels inputting to different muscles. Thus, equations (13.2)–(13.4) describe a generic component of a TPC $(T_1, T_2, \ldots, T_n)$, a DV $(V_1, V_2, \ldots, V_n)$, and a PPC $(P_1, P_2, \ldots, P_n)$. Rather than introduce subscripts $1, 2, \ldots, n$ needlessly, we merely note that our mathematical task is to show how the VITE circuit (13.2)–(13.4) behaves in response to a single GO function $G(t)$ if the initial value $T(0) - P(0)$ is varied. The variation of $T(0) - P(0)$ can be interpreted as the choice of a different setting for each of the components $T_i(0) - P_i(0), i = 1, 2, \ldots, n$. Alternatively it can be interpreted as the reaction of the same component to different target and initial position values on successive performance trials.

Figure 13.18 depicts a typical response to a faster-than-linear $G(t)$ when $T(0) > P(0)$. Although $T(t)$ is switched on suddenly to a new value T, $V(t)$ gradually increases-then-decreases, while $P(t)$ gradually approaches its new equilibrium value, which equals T. The rate of change $\frac{dP}{dt}$ of P provides a measure of the velocity with which the muscle group that quickly tracks $P(t)$ will contract. Note that $\frac{dP}{dt}$ also gradually increases-then-decreases with a bell-shaped curve whose decelerative portion $(\frac{d_2P}{dt_2} < 0)$ is slightly longer than its accelerative portion $(\frac{d_2P}{dt_2} > 0)$, as in the data described in Sections 13.8, 13.9, 13.12, and 13.13.

Figure 13.19 demonstrates movement synchrony and duration invariance. This figure shows that the V curves and the $\frac{dP}{dt}$ curves generated by widely different $T(0) - P(0)$ values and the same GO signal $G(t)$ are perfectly synchronous through time. This property is proved mathematically in Appendix 2. The simulated curves mirror the data summarized in Sections 13.12 and 13.13. These results demonstrate that the PPC output vector $(P_1(t), P_2(t), \ldots, P_n(t))$ from a VITE circuit dynamically defines a synergy which controls a synchronous trajectory in response to any fixed choice $(T_1, T_2, \ldots, T_n)$ of TPC, any initial positions $(P, (0), P_2(0), \ldots, P_n(0))$, and any GO signal $G(t)$.

13.23. Computer Simulation of Changing Velocity Profile Asymmetry at Higher Movement Speeds

The next simulations reproduce the data reviewed in Section 13.12

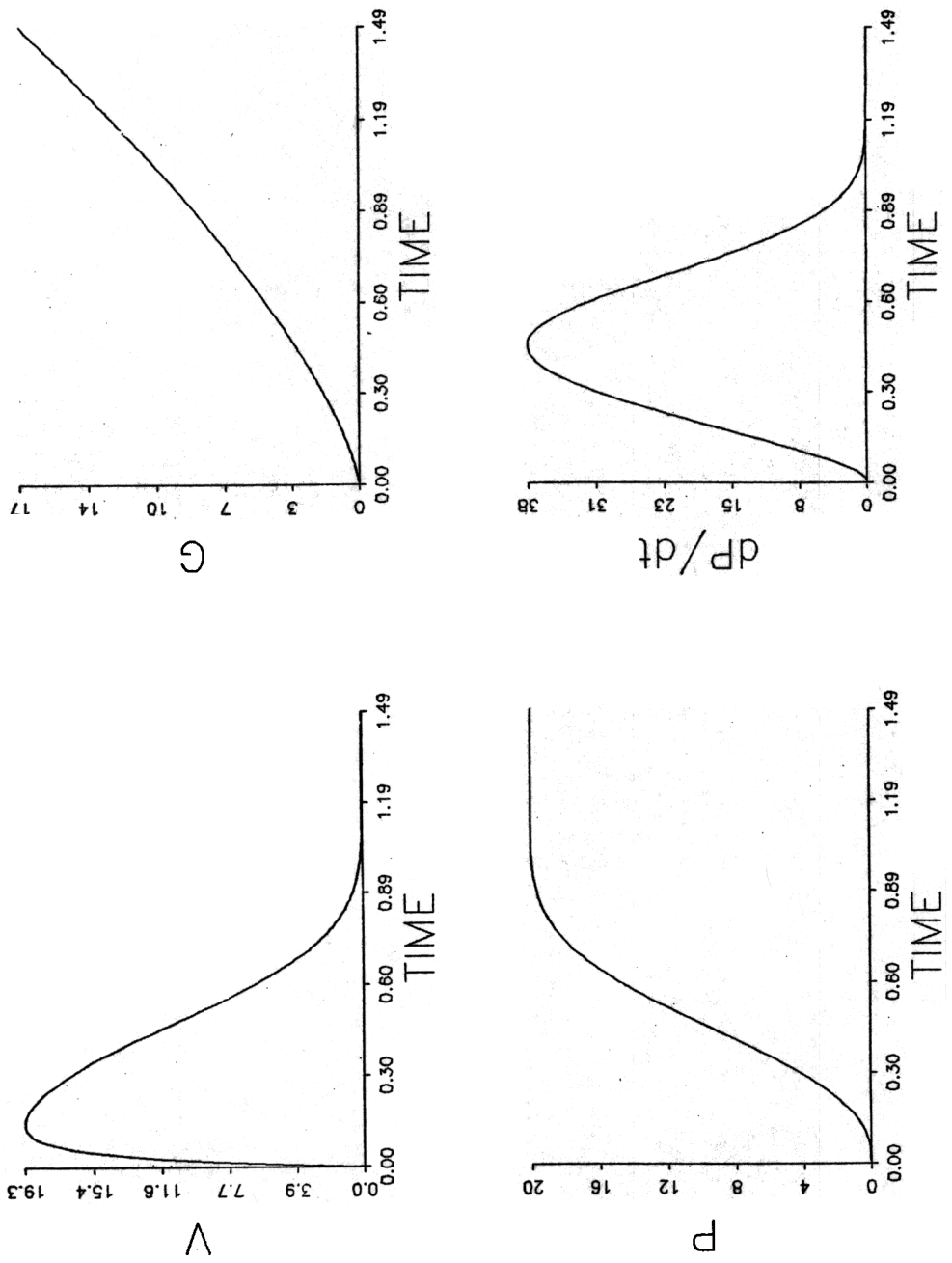

Figure 13.18. The simulated time course of the neural network activities V, G, and P during an 1100 msec. movement. The variable T (not plotted) had value 0 at $t < 0$, and value 20 thereafter. The derivative of P is also plotted to allow comparison with experimental velocity profiles. Parameters for equations (13.2), (13.3), (13.6): $\alpha = 30$, $n = 1.4$, $\beta = 1$, $\gamma = 0$.

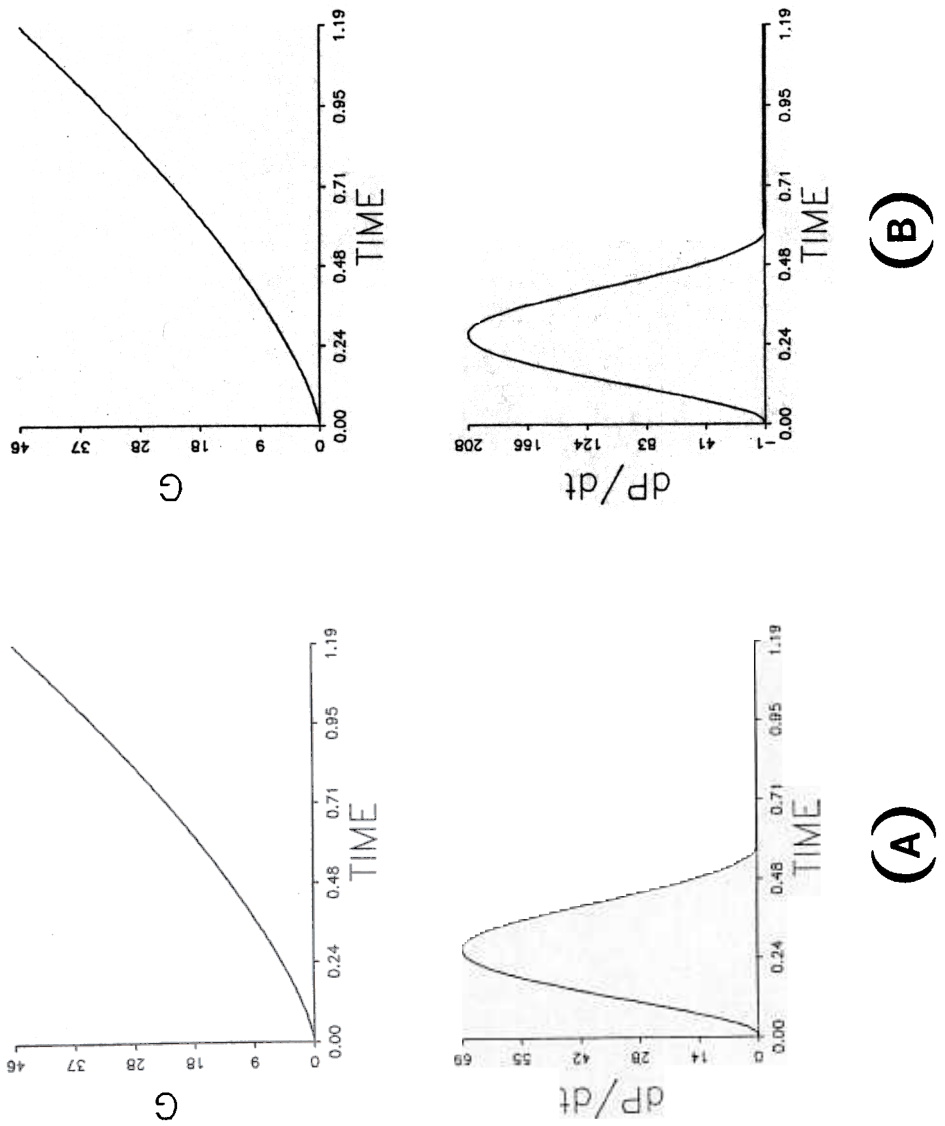

Figure 13.19. With equal GO signals, movements of different size have equal durations and perfectly superimposable velocity profiles after velocity axis rescaling. (A, B): GO signals and velocity profiles for 20 and 60 unit movements lasting 560 msec. (See Figure 13.18 caption for parameters.)

concerning the greater symmetry of velocity profiles at higher movement velocities. In these simulations, the initial difference $T(0) - P(0)$ between TPC and PPC was held fixed and the GO amplitude G_0 was increased. Figure 13.20a–c shows that the profile of $\frac{dP}{dt}$ becomes more symmetric as G_0 is increased. At still larger G_0 values, the direction of asymmetry reversed; that is, the symmetry ratio exceeded .5, as in the data of Zelaznik, Schmidt, and Gielen (in press). Figure 13.20d shows that if both the time axis t and the velocity axis $\frac{dP}{dt}$ are rescaled, then curves corresponding to movements of the same size at different speeds can approximately be superimposed, except for the mismatch of their decelerative portions, as in the data summarized in Section 13.12.

13.24. Why Faster-than-Linear or Sigmoid Onset Functions?

The parametric analysis of velocity profiles in response to different values of $T(0) - P(0)$ and G_0 led to the choice of a faster-than-linear or sigmoid onset function $g(t)$. In fact, the faster-than-linear onset function should be interpreted as the portion of a sigmoid onset function whose slower-than-linear part occurs at times after $P(t)$ has already come very close to T.

Figure 13.21 shows what happens when a slower-than-linear $g(t) = t(\beta + t)^{-1}$ or a linear $g(t) = t$ is used. At slow velocities (small G_0), the velocity profile $\frac{dP}{dt}$ becomes increasingly asymmetric when a slower-than-linear $g(t)$ is used. At a fixed slow velocity, the degree of asymmetry increases as the slower-than-linear $g(t)$ is chosen to more closely approximate a step function. A linear $g(t)$ leads to an intermediate degree of asymmetry. A faster-than-linear, or sigmoid, $g(t)$ leads to slight asymmetry at small values of G_0 as well as greater symmetry at large values of G_0. A sigmoid $g(t)$ can be generated from a sudden onset of GO signal if at least two cell stages average the GO signal before it gates $[V]^+$ in (13.3). A sigmoid $g(t)$ contains a faster-than-linear part at small values of t, and an approximately linear part at intermediate values of t. Thus a sigmoid $g(t)$ can generate different degrees of asymmetry depending upon how much of the total movement time occurs within each of these ranges.

We have also simulated a VITE circuit using sigmoid GO signals whose rate of growth increases with the size of the GO amplitude. Such covariation of growth rate with amplitude is a basic property of neurons which obey membrane, or shunting, equations (Grossberg, 1970, 1973, 1982a; Sperling and Sondhi, 1968). Such a sigmoid GO signal $G(t)$ can be simply defined as the output of the second neuron population in a chain of shunting equations perturbed by a step function input with amplitude G_0. Thus, let

$$G_0(t) = \begin{cases} G_0 & \text{if } t \geq 0 \\ 0 & \text{if } t < 0 \end{cases} \tag{13.7}$$

$$\frac{d}{dt}G_1 = -AG_1 + (B - G_1)G_0 \tag{13.8}$$

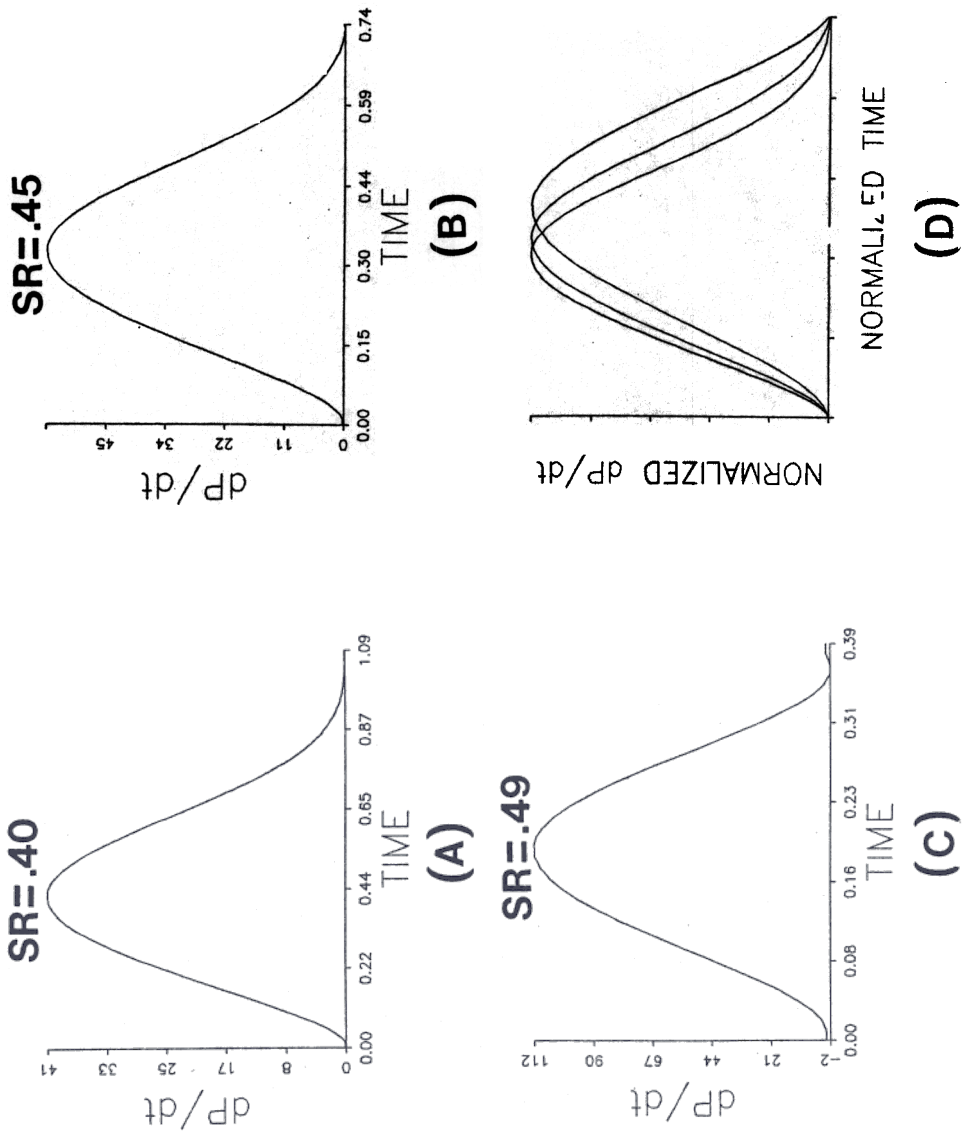

Figure 13.20. (A, B, C): Velocity profiles associated with a slow, medium, and fast performance of a 20 unit movement. Each SR value gives the trajectory's *symmetry ratio*; that is, the time taken to move half the distance, $.5(T(0) - P(0))$, divided by the total movement duration, MT. These ratios indicate progressive symmetrization at higher speeds. (D): The velocity profiles shown in (A), (B), and (C) are not perfectly superimposable. (See Figure 13.18 for parameters.)

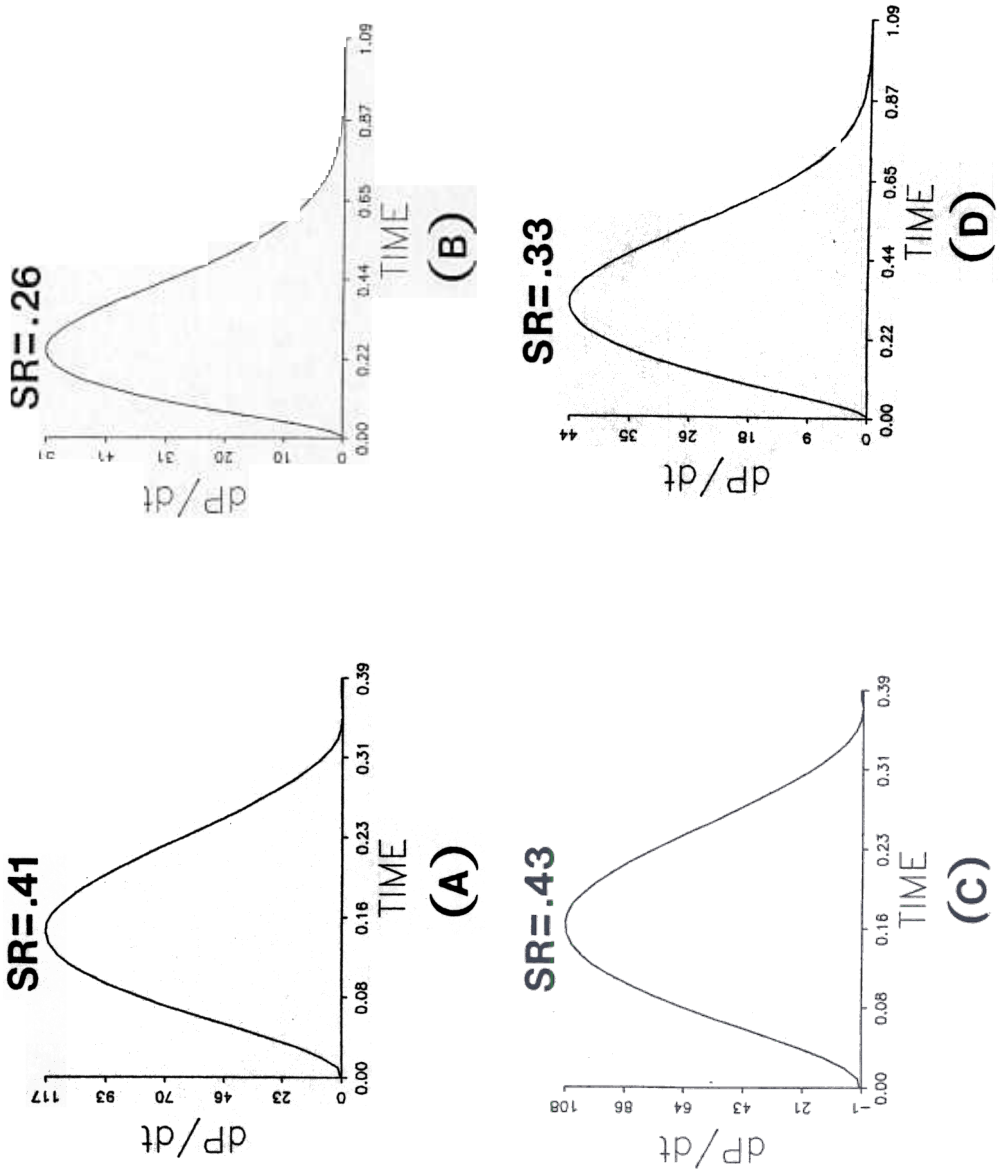

Figure 13.21. (A, B): Velocity profiles for a slow and a fast movement with a slower-than-linear $g(t)$: $\alpha = 30$, $n = 1$, $\beta = 1$, $\gamma = 1$. (C, D): Velocity profiles for a slow and a fast movement with a linear $g(t)$: $\alpha = 30$, $n = 1$, $\beta = 1$, $\gamma = 0$. (SR = symmetry ratio.)

and

$$\frac{d}{dt}G_2 = -AG_2 + (B - G_2)G_1. \tag{13.9}$$

Then $G_2(t)$ is a sigmoid function of the desired shape. The GO signal $G(t)$ can be set equal to $G_2(t)$, as we did, or even to a sigmoid signal $f(G_2(t))$ of $G_2(t)$. A typical result is shown in Figure 13.22. In the series of simulations exemplified by Figure 13.22, the range of symmetry ratios, namely .44–.50 was similar to that found in Figure 13.19 using a faster-than-linear signal function. Final choice of a best-fitting $G(t)$ awaits a more direct experimental determination of the PPC profile through time.

13.25. Computer Simulation of Velocity Amplification during Target Switching

Velocity amplification by up to a factor of three can be obtained by switching to a new value of T while a previously activated GO signal is still on. Figure 13.23 demonstrates this effect by comparing two computer simulations. In the first simulation, onset of $T(t)$ and $g(t)$ were both synchronous at time $t = 0$ (Figure 13.23a). In the second simulation, onset of $g(t)$ preceded onset of $T(t)$ by a time equivalent to about 300 msec (Figure 13.23b). Note the much higher peak velocity (235 versus 102) attained in Figure 13.23b. This effect, which matches the "anomalous" velocity multiplication observed in the target-switching experiments of Georgopoulos *et al.* (1981), is due to the prior build-up of the GO signal during response execution.

In the ensuing sections, computer simulations will be compared with a variety of data which were not reviewed in the preceding sections.

13.26. Reconciling Staggered Onset Times with Synchronous Termination Times

Within the context of a target-switching experiment, velocity amplification may appear to be a paradoxical property. On the other hand, such a property has an adaptive function in the many situations where a hand will fail to reach a moving target unless it both changes direction and speeds up. In addition, we now show that the same mechanism can generate synchronous termination times of synergetic muscle components which may individually start to move at staggered onset times.

The need for this latter property has recently been emphasized by a study of Hollerbach, Moore, and Atkeson (1986), who showed that nearly straight movement paths can result from muscle coordinate planning if the onset times of muscles acting at different joints are appropriately staggered *and* if all the muscles reach their final positions synchronously. Their study did not, however, explain how a neural mechanism could generate synchronous muscle offsets despite staggered muscle onsets.

We now show that the posited interaction of a growing GO signal with components of a DV that may be switched on at different times automatically generates synchronous offsets as an emergent property of

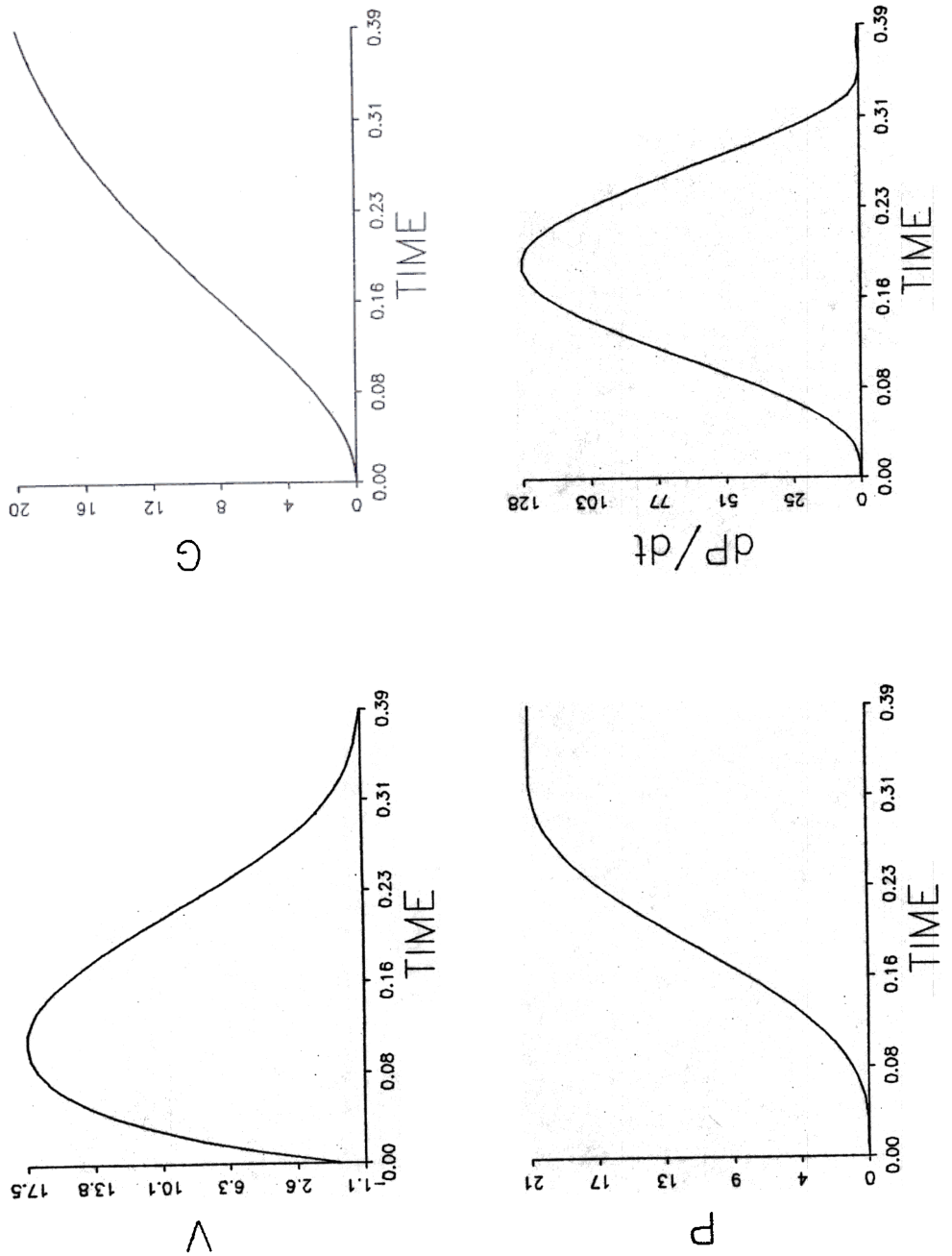

Figure 13.22. Simulated time course of neural network activities and $\frac{dP}{dt}$ for a 350 msec movement. Note the S-shaped growth in G (sigmoid GO signal). Parameter values for equations (13.2), (13.3), (13.8), (13.9): $\alpha = 25$, $A = 1$, $B = 25$.

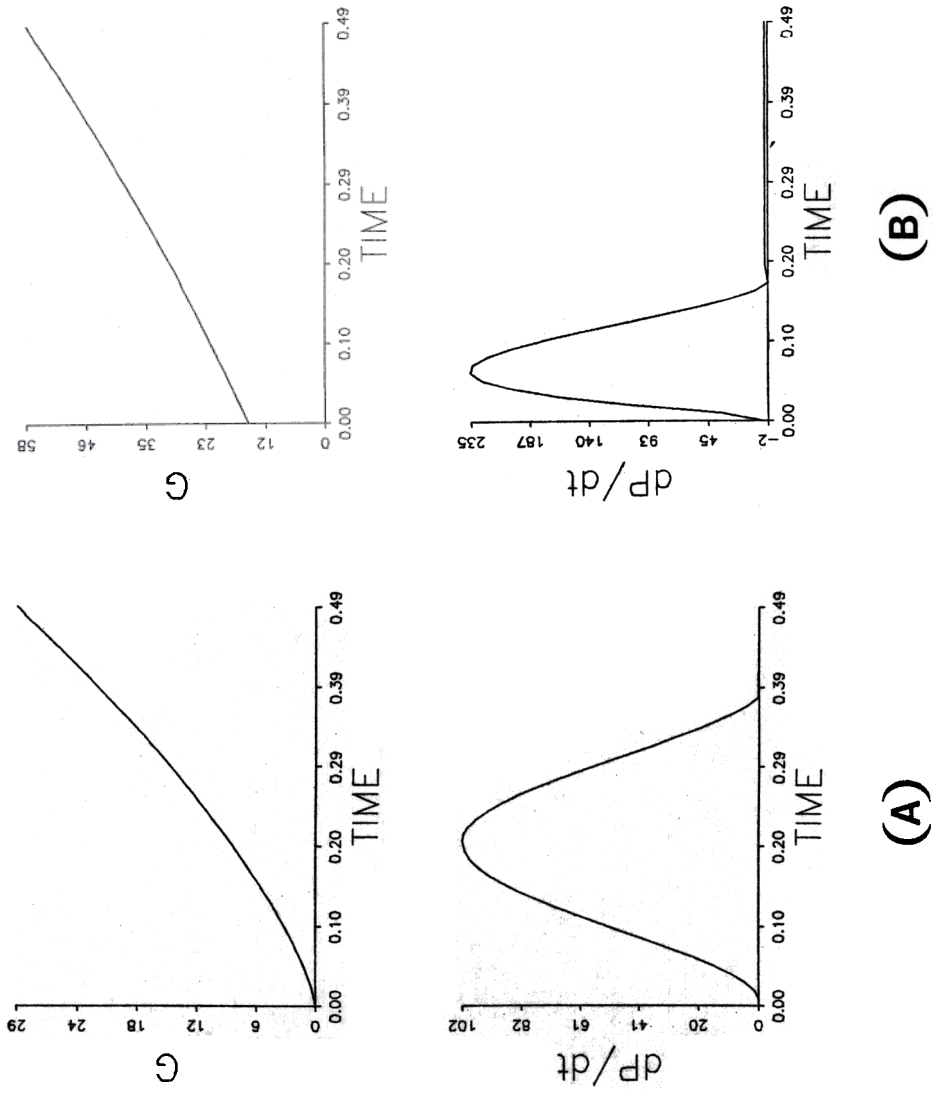

Figure 13.23. A much higher peak velocity is predicted by the model whenever a target is activated after the GO signal has already had time to grow. (A): The control condition, in which T and the GO signal growth process are activated synchronously. (B): Same T as in (A), but here T was activated after $G(t)$ had been growing for 300 msec. (See Figure 13.18 for parameters.)

the VITE circuit. Thus the interaction of a GO signal with a DV both helps to linearize the paths generated by individual TPC's and, as in the target-switching experiments, enables the hand to efficiently track a moving target by quickly reacting to read-out of an updated TPC.

Figure 13.24 depicts the results of four blocks, labelled I, II, III, and IV, of computer simulations. Each block represents the onset time, offset time, and duration of three simulations. In the leftmost simulations of each block, onset of a DV component and a GO signal were synchronous. In the other two simulations of each block, a different DV component was read-out at successively longer delays with respect to the onset time of the GO signal. Due to duration invariance (Appendix 2), the results are independent of the initial sizes of the $T(0) - P(0)$ values of these components.

The four blocks (I, II, III, IV) correspond to four increasing values of the GO amplitude G_0 $(10, 20, 40, 80)$. The approximate invariance of termination times across components with different onset delays is indicated by the nearly equal *heights* reached by all the bars within the block. The different *lengths* of bars within each block show that less time is needed to update those components whose onset times are most delayed. Thus, in block I, all the components terminate almost synchronously even though their onset times are staggered by as much as 26% of the total movement time. In block II, almost synchronous terminations occur even though onset times are staggered by as much as 39% of the total movement time. At very large choices of G_0 (blocks III and IV), synchrony begins to gently break down because the earliest components have executed over 50% of their trajectories before later components even begin to move. These and other results in the article suggest the critical importance of experimentally testing the existence and predicted properties of GO–DV interactions, notably the predicted correlations between the temporal evolution of the GO signal and the DV.

13.27. Computer Simulation of the Inverse Relation between Duration and Peak Velocity

Each curve depicted in Figure 13.25a summarizes a series of simulations in which $T(0) - P(0)$ was held constant while G_0 was varied . In this way, a series of velocity profiles were generated whose peak velocities differed even though their trajectories traversed the same distance. The duration of each movement was computed by measuring the interval between velocity profile zero crossings. The different curves in Figure 13.25a used different values of the distance parameter $T(0) - P(0)$.

These curves mirror the data of Lestienne (1979) summarized in Figure 13.25b. Figure 13.25b plots agonist burst duration against peak velocity. The overall shapes of the plots of simulated durations (Figure 13.25a) and agonist burst durations (Figure 13.25b) as a function of peak velocity are similar. This similarity reinforces the postulate that the VITE circuit operates in agonist-antagonist muscle coordinates (Sections 13.3 and 13.20). It also suggests that the relationship between VITE circuit outputs, mo-

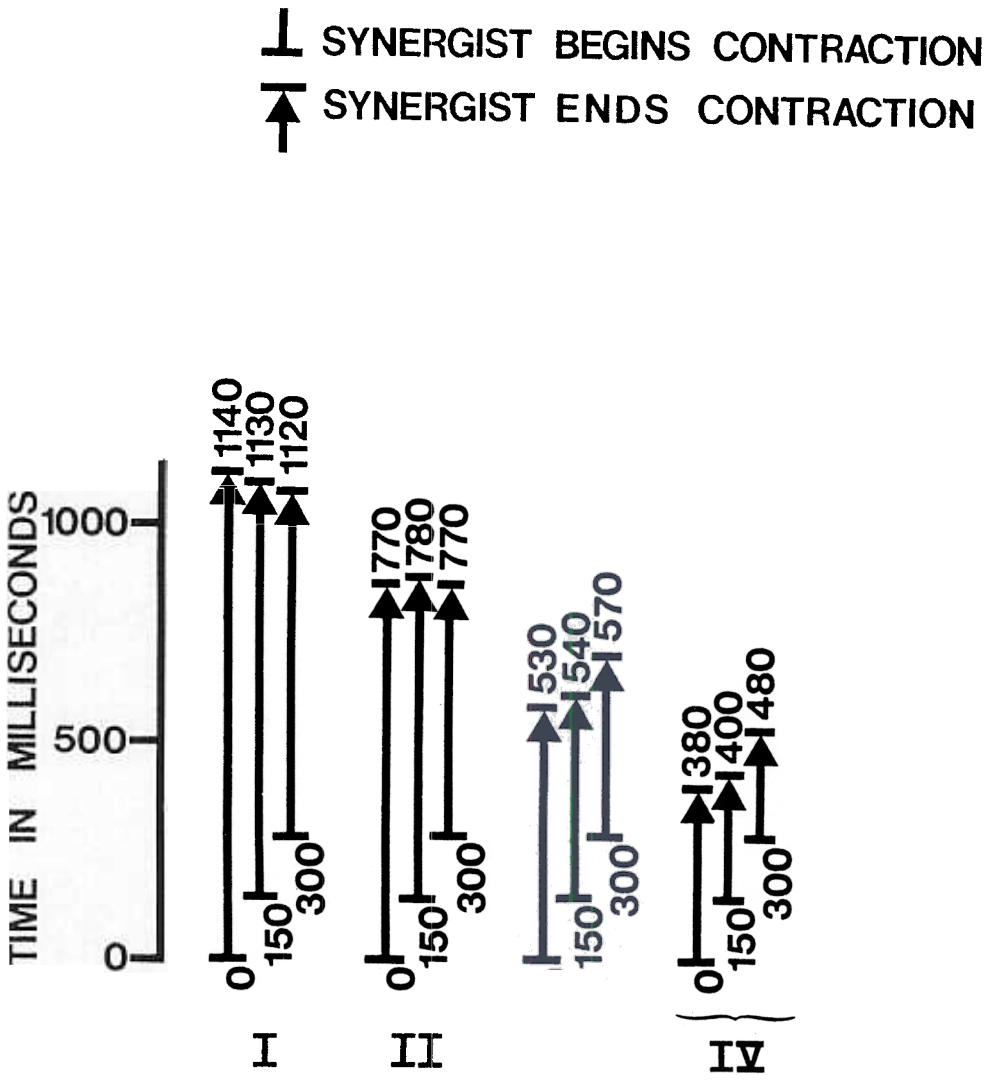

Figure 13.24. Simulation results showing automatic VITE circuit compensation for contraction-onset-time staggering across components of a synergy. Each block (I, II, III, IV) shows results for a different value (10, 20, 40, and 80, respectively) of the GO signal scalar, G_0. (See Figure 13.18 for parameters.)

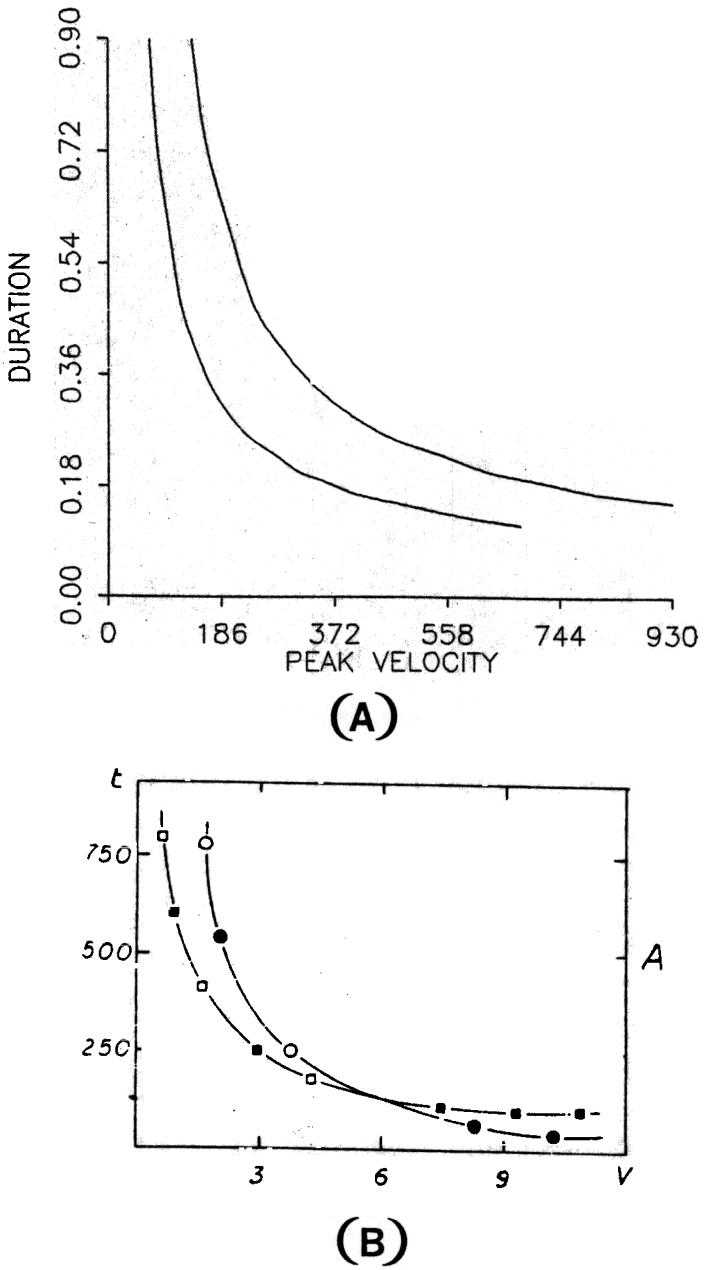

Figure 13.25. (A): Simulation of movement duration (sec) as a function of peak velocity (deg/sec) for a 30° (lower curve) and a 60° (upper curve) movement. (See Figure 13.18 for parameters.) (B): Data on agonist burst duration (squares) and antagonist burst onset-time (dots) as a function of peak velocity (rad/sec) for a 60° movement. Reprinted with permission from Lestienne (1979).

toneuron inputs, and actual muscle activities might be relatively simple (Bullock and Grossberg, 1988b).

Nevertheless, two caveats deserve mention. First, were Figure 13.25a a plot of movement duration (MT) against *mean* velocity ($\overline{V}$), it would necessarily have the shape shown, since by definition,

$$MT = \frac{D}{\overline{V}}, \tag{13.10}$$

where D denotes the distance. Multiplying by different values of D generates a family of curves similar in shape to those shown in Figure 13.25a. The VITE model generates the curve in Figure 13.25a because mean velocity and peak velocity are strongly correlated in these VITE trajectories due to the duration invariance described in Section 13.22.

The second caveat acknowledges that the VITE circuit cooperates with several other circuits to generate a controllable trajectory in response to unexpected loads and to variable velocities (Bullock and Grossberg, 1988b). For example, during medium and high speed movement, the duration of the initial agonist burst may be only one fourth the duration of the corresponding movement. If we assume that the PPC updating process consumes most of the movement time, then these short duration EMG bursts are further evidence that the PPC stage must not be identified with—and must be higher in the outflow channel than—the spinal motorneurons whose suprathreshold activities are directly reflected in the EMG bursts.

This conclusion is consonant with available data on the genesis of EMG burst patterns. In vivo, EMG activites are often sculpted into multiphasic burst patterns by several subnetworks that converge on and embed the spinal motorneurons. In particular, during high-speed movements, muscle changes lag behind neural changes early in response development. This leads to registration of "lag errors" at model regulatory circuits (Bullock and Grossberg, 1988b; Feldman, 1986; Ghez and Martin, 1982; Grossberg and Kuperstein, 1986), including the stretch reflex and cerebellar circuits, which translate these error signals into large agonist activations and antagonist inhibitions. If the large agonist activations accelerate the limb so much that it begins to overshoot the intended position, this overshoot is registered as an error opposite in sign to the initial lag error, and the result is a large antagonist braking activity in concert with agonist inhibition. Such braking may slow the movement enough that a smaller lag-error is once again registered. Though this results in a second agonist burst, and transient antagonist inhibition, this last phasic modulation fades quickly and gives way to the tonic EMG pattern required to hold the arm at the final postural position. A similar analysis may be given for isometric contractions.

TABLE 13.1
FOR FIXED DURATION (MT), ERROR GROWS IN PROPORTION TO DISTANCE

MT	DISTANCE	ERROR
.56	10	.084
.56	20	.170
.56	40	.349
.56	80	.700

13.28. Speed-Accuracy Trade-off: Woodworth's Law and Fitts' Law

The VITE Model circuit predicts a speed-accuracy trade-off which quantitatively fits the classical laws of Woodworth (1899) and of Fitts (1954). The existence of a speed-accuracy trade-off *per se* can be understood by considering the role of the rate parameter α in equation (13.1). The case of an overshoot error is considered for definiteness.

Given *any* finite value of the averaging rate α in equation (13.2), $V(t)$ takes some time to react to changes in $P(t)$. In particular, even if $P(t) = T$ at a given time $t = t_0$, $V(t)$ will typically require some extra time after $t = t_0$ to decrease to the value 0, and by (13.3) $P(t)$ will continue to increase during this extra time. If α is very large, $V(t)$ can approach 0 quickly. Consequently, by (13.3), $V(t)$ will not allow $P(t)$ to overshoot the target value T by a large amount. On the other hand, given *any* choice of α, the *relative* amount whereby $P(t)$ overshoots the target T depends upon the size of the GO amplitude G_0. This is true because a larger value of G_0 causes $P(t)$ to increase faster, due to (13.3), and thus $P(t)$ can approach T faster. In contrast, $V(t)$ can only respond to the rapidly changing values of $T - P(t)$ at the constant rate α. As a result, $V(t)$ tends to be larger at a time $t = t_0$ when $P(t_0) = T$ if G_0 is large than if G_0 is small. It therefore takes $V(t)$ longer to equal 0 after $t = t_0$ if G_0 is large. Thus $P(t)$ overshoots T more if G_0 is large. This covariation of amount of overshoot with overall movement velocity is a speed-accuracy trade-off.

Fitts' Law, as described in equation (13.1), relates movement time (MT), distance (D), and target width (W). The target width may be thought of as setting the criterion for what counts as an error. The law may be given two complementary readings. The first notes that for a fixed movement time, error grows in proportion to amplitude. This component of the law was discovered by Woodworth (1899). Table 13.1 presents simulation results based on the same parameter choices used in Figure 13.18. The results show that, in a parameter range where model overshoot errors occur, the model's error also grows in proportion to amplitude. In these simulations, G_0 was held fixed and $T(0) - P(0)$ was varied.

The second way of reading the law notes that in order to maintain

TABLE 13.2
FOR FIXED ERROR LEVEL, DURATION (MT) GROWS LINEARLY WITH DISTANCE DOUBLING

ERROR	DISTANCE	MT
.059	2	.39
.057	4	.49
.058	8	.59
.059	16	.70
.057	32	.80
.059	64	.91

a fixed absolute error size, or to fall within a target zone of fixed width, while increasing movement distance, it is necessary to allow more time for completing the movement. In particular, every doubling of distance will add a constant amount, b, to the time needed to perform the movement with the same level of accuracy. Allowing less than b more time for a movement of twice the distance will lead to a less accurate movement.

Table 13.2 presents the results of a simulation (parameters as in Figure 13.18) in which the rate parameter α was small enough that modest error resulted even at the smallest distance, or initial value of $T(0) - P(0)$, that was tested, namely a distance of 2 units. Then the distance $T(0) - P(0)$ was repeatedly doubled, and the value of G_0 progressively decreased, such that the error level was held approximately constant. As can be seen, movement time increased approximately linearly with each doubling of distance, as required by a logarithmic relation between MT and D. It should be noted that the "errors" shown in Tables 13.1 and 13.2 are defined relative to a mathematical point, that is a target having zero width along the direction of motion. If subjects adjust their GO signal so that expected error is no greater than the width of a physical target, then by choosing a TPC corresponding to the near-side of the target, they can produce the "errorless" movements required in the Fitts task. The model's striking replication of the laws of Woodworth and Fitts, together with its other successes in experimental results, increases our confidence that the VITE Model captures some of the basic neural design principles that underly trajectory generation *in vivo*.

Woodworth's Law is a consequence of duration invariance in the model. This can be seen from the mathematical analysis provided in Appendix 2. There it is proved that the PPC value $P(t)$ can be written in the form

$$P(t) = P(0) + (T(0) - P(0)q(t)) \qquad (13.11)$$

given *any* continuous GO signal $G(t)$. In (13.11), $T(0) - P(0)$ represents the amount of contraction, or "distance" to be moved, that is mandated by the TPC value $T(0)$ and the initial PPC value $P(0)$. Function $q(t)$

is independent of $P(0)$ and $T(0)$. By (13.11), $P(t)$ approaches $T(0)$ as $q(t)$ approaches 1, and $P(t)$ overshoots or undershoots if $q(t)$ approaches a value greater or less than 1, respectively. Since $q(t)$ is multiplied by $T(0)-P(0)$, the amount of error (undershoot or overshoot), is proportional to distance, as in Woodworth's Law.

Whereas the proof of Woodworth's Law is a general consequence of duration invariance in the model, Fitts' Law has been mathematically proved in only one case as of the present time (Appendix 1), although our computer simulations demonstrate that it occurs with greater generality. In this case, the GO signal $G(t)$ switches on from value 0 at times $t < 0$ to the constant value $G_0 > 0$ at times $t \geq 0$. In addition, G_0 is chosen sufficiently large to generate overshoot errors. In particular, when $4G_0 > \alpha$,

$$MT = \frac{2}{\alpha} \log\left(\frac{T(0) - P(0)}{E}\right) \tag{13.12}$$

where E is the amount of overshoot error in the VITE command.

These instances of Woodworth's Law and Fitts' Law are generated by the VITE circuit itself, without the intervention of visual feedback. A number of authors have commented upon the applicability of these laws when visual feedback is inoperative. For example, Keele (1982, pp.152–153) has written: "What is the underlying nature of the movement system that yields Fitts' Law? ... One factor is the intrinsic accuracy of the motor control system when visual feedback is unavailable. When the eyes are closed during a movement (or the lights are turned off), an average movement will miss target by about 7% of the total distance moved." Schmidt (1982, pp.253–254) summarized error functions for sighted and blind movements across various movement times from studies of Keele and Posner (1968) and Zelaznik, Hawkins, and Kisselburgh (1983). A clear speed-accuracy trade-off was observed. Meyer, Smith, and Wright (1982, p.450) have reviewed data comparing the initial impulse phase of a movement, where visual feedback is unimportant, with the subsequent current-control phase, where visual feedback may be used to improve accuracy. They noted that "the initial-impulse phase was found to contribute directly to the speed-accuracy trade-off. Even when subjects had to perform with their eyes closed and relied on just this phase to execute their movements, they still produced a trade-off ... models that attempt to account for the speed-accuracy trade-off ... must include mechanisms that modulate the trade-off during the initial-impulse phase, not just during the current-control phase." The VITE circuit's ability to reproduce both Woodworth's Law and Fitts' Law as emergent properties of the PPC updating process satisfies this requirement.

It should be emphasized that the VITE circuit is also capable of generating a PPC that approaches the TPC without error in some parameter ranges (Appendix 1). In these parameter ranges, an undershoot error will occur if the GO signal is prematurely terminated or if the effects of small DV signals get lost in ambient cellular noise. A range effect has also been reported (Georgopoulos, 1986, p.151) such that "subjects tended to over-

shoot the target in small movements (2.5 cm) and to undershoot in large movements (40 cm)." A number of factors may influence this result. For example, during high speed small movements, auxiliary circuits for controlling the arm's inertial effects may not have a sufficient opportunity to act (Grossberg and Kuperstein, 1986, Chapters 3 and 5). During large movements, the distance to be moved may be visually underestimated, thereby leading to instatement of an incorrect TPC. The choice of GO signal amplitude as a function of target distance may contribute to the range effect. The relative importance of such factors will be easier to assess as new experiments and the theory are progressively elaborated with the aid of the quantitative VITE circuit analysis that is provided herein.

Even the definition of what constitutes a movement "error" during ecologically useful motor behavior deserves further commentary. For example, Carlton (1979) asked subjects to keep their movement errors below 5 percent. Subjects typically chose a two-part movement strategy whose first velocity component undershot the target, and whose second velocity component made the final approach to the target at a much lower speed. Such results suggest that subjects found it easier to achieve greater accuracy by breaking up the movement into parts than by launching the movement ballistically over the full distance. The first movement part, albeit strictly speaking an "undershoot error", provides the occasion for updating TPCs and choosing small GO signals during the final part of the movement, thereby achieving high accuracy without too great an increase in total movement duration. Because GO signal adjustments may also be necessary during the final components of such composite movements, these components may also obey a speed-accuracy tradeoff, as Carlton (1979) found.

13.29. Computer Simulation of Peak Acceleration Data

Bizzi *et al.* (1984) measured the peak accelerations of medium-speed forearm movements by monkeys. They considered movements around the elbow that swept out 20° and 60°. A computer simulation is compared with their data in Table 13.3. In order to make this comparison, we scaled 1 time unit in our simulation to equal 10 msec. We then chose two values of the GO amplitude parameter G_0 which generated trajectories of duration approximately equal to 554 msec. and 692 msec., respectively. Due to duration invariance (Section 13.22), the same durations obtain given these choices of G_0 over a wide range of choices of the distance measure $T(0) - P(0)$. The fact that movements were 20° or 60° was translated into the constraint that the $T(0) - P(0)$ value corresponding to the smaller choice of G_0 must be chosen three times larger than the $T(0) - P(0)$ value corresponding to the larger choice of G_0. Then we searched for values of $T(0) - P(0)$ that gave the best fit to the peak acceleration data subject to this constraint.

The result is compared in Table 13.3 with the data, and with the fit of the Minimum-Jerk Model of Hogan (1984). The VITE Model fit these data substantially better than the Minimum-Jerk Model. The values associated with the VITE$^+$ model indicate that a perfect fit can be

TABLE 13.3
A COMPARISON OF THREE MODELS' ABILITIES TO PREDICT DATA ON PEAK ACCELERATION ($\ddot{P}$)

DISTANCE	MT	PEAK $\ddot{P}$	PEAK $\ddot{P}$ SOURCE
20°	.554	$397°/sec^2$	Bizzi *et al.* (1984)
60°	.692	$1130°/sec^2$	(experimental data)
20°	.554	$376°/sec^2$	Minimum-jerk model
60°	.692	$722°/sec^2$	(simulation)
20°	.554	$394°/sec^2$	VITE model
60°	.692	$854°/sec^2$	(simulation)
20°	.554	$396°/sec^2$	VITE$^+$ model
60°	.692	$1127°/sec^2$	(simulation)

obtained (with Figure 13.18 parameters) if DV readout to the shunting stage, rather than being instantaneous, occurs over a brief interval whose length is proportional to the size of the DV.

As noted in Section 13.12, the Minimum-Jerk Model also erroneously predicts a symmetric velocity profile, at least at the level of the central controller. Moreover, it is hard to see how this model could explain the velocity amplification that occurs during target switching (Section 13.11). Finally, the Minimum-Jerk Model does not contain any representation that may be compared with the existence of vector cells or with the manner in which vector cell activities are integrated into outflow movement commands (Section 13.13). We therefore believe that the VITE Model provides a better foundation for developing a quantitative neurally-based theory of arm movements than does the Minimum-Jerk Model. The VITE model, in addition to the model circuits developed in Grossberg and Kuperstein (1986), also provides a mechanistic neural explanation of some of the types of invariant behaviors for whose analysis the task dynamics approach to motor control was developed (Saltzman and Kelso, 1983).

13.30. Updating the PPC using Inflow Signals during Passive Movements

Despite these successes, the VITE Model as described above is far from complete. In this section, a solution of one additional design problem is outlined. Bullock and Grossberg (1988b) suggest solutions of a number of the other design problems whereby a VITE circuit can effectively move an arm of variable mass subjected to unexpected perturbations at variable velocities through a Newtonian world.

In Section 13.6, we noted that inflow signals are needed to update the PPC during a passive movement. For example, Gellman, Gibson, and Houk (1985) have described cells in the cat inferior olive that are sensitive to passive body displacement but not to active movement, and Clark, Burgess, Chapin, and Lipscomb (1985) have analysed muscle proprioceptive contributions to position sense during passive finger movements in humans. Two basic problems motivate our model of PPC updating by inflow signals. First, the process of updating the PPC during passive movements must continue until the PPC registers the position coded by the inflow signals. Thus a difference vector of inflow signals minus PPC outflow signals updates the PPC during passive movements. We denote this difference vector by DV_p to distinguish it from the DV which compares TPC's with PPC's. At times when $DV_p = 0$, the PPC is fully updated. Although the DV_p is not the same as the DV which compares a TPC with a PPC, the PPC is a source of inhibitory signals, as will be seen below, in computing both difference vectors.

Second, PPC outflow signals and inflow signals may, in principle, be calibrated quite differently. We will show how corollary discharges of the PPC outflow signals are adaptively recalibrated until they are computed in the same numerical scale as the inflow signals to which they are compared. We also show that this adaptive recalibration mechanism automatically computes a DV_p which updates the PPC by just the correct amount.

Figure 13.26 schematizes a model circuit for adaptively computing this DV_p. We call this circuit the *passive update of position (PUP) model.* In Figure 13.26, the PPC sends inhibitory corollary discharge signals towards the outflow-inflow match stage where the inflow signals are registered. It is assumed that this stage is inhibited except when the movement command circuit is inactive. A simple way to achieve this property is to assume that the GO signal in the movement command circuit inhibits the outflow-inflow match stage, as in Figure 13.25. Thus the mismatches of outflow and inflow signals that occur during every active movement do not erroneously update the outflow-inflow match stage. In addition, the GO signal is assumed to inhibit learning at the LTM traces which multiply the PPC signals on their way to the outflow-inflow match stage.

This assumption is consistent with arm movement results of Evarts and Fromm (1978) which showed greater modulation of vector cells in precentral motor cortex by inflow signals during small slow movements than during posture, and strongly attenuated modulation during large fast movements. In the model, the amount of attenuation increases with the size of the GO signal. The gating signal which attenuates the inflow process may be a nonlinear (e.g., sigmoid) function of the GO signal. Parametric analysis of the degree of inflow attenuation as a function of overall active movement speed would provide valuable information about the form of this hypothesized gating signal.

After a movement is over, both the outflow-inflow match stage and the LTM traces are released from inhibition. Typically, the PPC represents the same position as the inflow signals, but perhaps in a different numerical

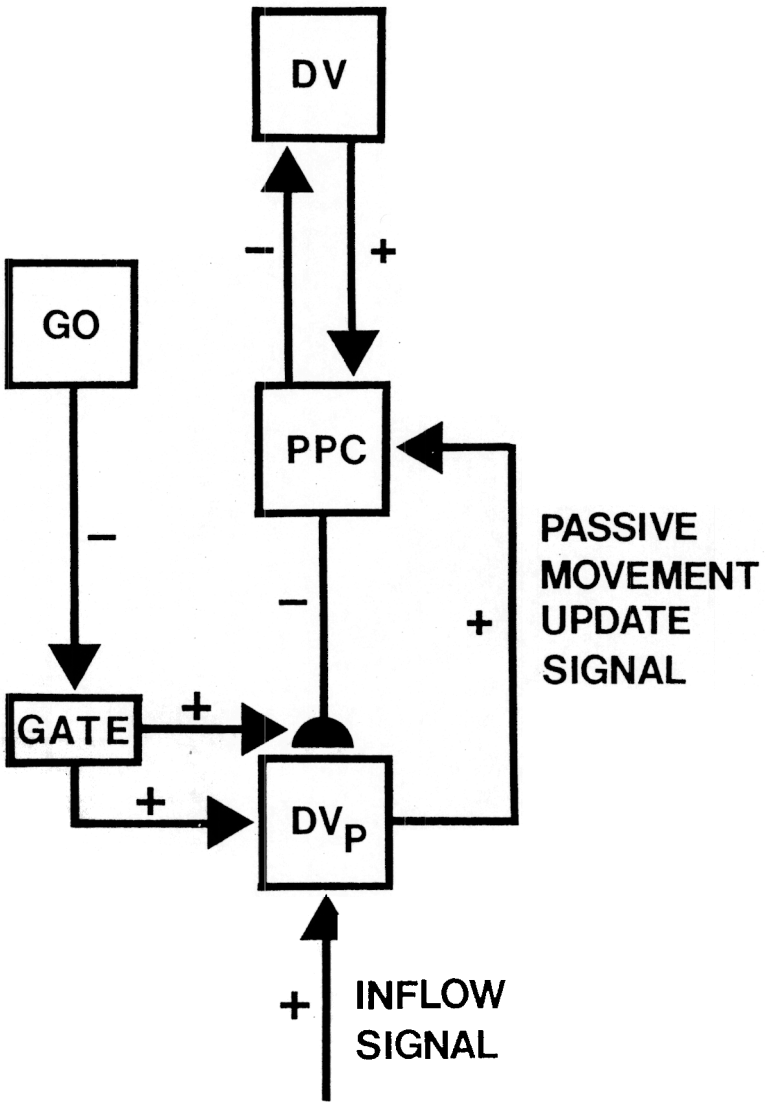

Figure 13.26. A passive update of position (PUP) circuit. An adaptive pathway $PPC \rightarrow DV_P$ calibrates PPC-outflow signals in the same scale as inflow signals during intervals of posture. During passive movements, output from DV equals zero. Hence the passive difference vector DV_P updates the PPC until it equals the new position caused by any passive movements that may occur due to the application of external forces.

scale. The learning laws described in Appendix 3 define LTM traces which change until the PPC *times* the LTM trace equals the inflow signal. After a number of such learning trials during stable posture, $DV_p = 0$ and the PPC signals are rescaled by the LTM traces to correctly match the inflow signals.

During a passive movement, the PPC does not change, but the inflow signal may change. If the DV_p becomes positive, it causes an increase in the PPC until the DV_p decreases to 0 and the PPC is correctly updated by the inflow signals. If the DV_p becomes negative, then the DV_p of the opponent muscle can decrease the PPC until a match again occurs.

13.31. Concluding Remarks

The present article introduces a circuit for automatically translating a target position command into a complete movement trajectory via a mechanism of continuous vector updating and integration. A wide variety of behavioral and neural data can be quantitatively explained by this mechanism. The model also provides a foundation for clarifying some of the outstanding classical issues in the motor control literature, highlights the relevance of learning constraints upon the design of neural circuitry, and may be viewed as a specialized version of a more general architecture for movement control.

The VITE circuit and the PUP circuit do not, however, exhaust the total neural machinery that is needed for the control of arm movements. Mechanisms for properly timed sequential read-out of TPC's in a serial motor plan, such as during reaching and grasping or during a dance (Grossberg and Kuperstein, 1986, Chapter 9), for adaptive linearization of a nonlinear muscle plant (Grossberg and Kuperstein, 1986, Chapter 5), and for automatically or predictively adapting to the inertial properties generated by variable loads and velocities (Bullock and Grossberg, 1988b) also form essential parts of the arm control system. When all of these systems are joined together, however, one can begin to understand quantitatively how the arm system achieves its remarkable flexibility and versatility, and can begin to build a new type of biologically inspired adaptive robot whose design is qualitatively different from the algorithms offered by traditional approaches to artificial intelligence.

APPENDIX 1

Bell-Shaped Velocity Profile, Fitts' Law, and Staggered Onset Times

This Appendix solves the system of equations

$$\frac{d}{dt}V = \alpha(-V + T - P) \tag{A1}$$

$$\frac{d}{dt}P = G[V]^+ \tag{A2}$$

under the simplifying assumption that the GO signal G is a step function. Then the system can easily be integrated to demonstrate some basic properties.

In many situations, the system starts out in an equilibrium state such that the PPC equals the TPC. Then a new TPC is switched on and the system approaches a new equilibrium. Before the new TPC is switched on, $P = T$ in (A1). Since the system is at equilibrium, $\frac{d}{dt}V = 0$. Thus, by (A1), it also follows that $V = 0$ under these circumstances.

Suppose that a new TPC value is switched on at time $t = 0$. If the system represents an agonist muscle, then $T(0) > P(0)$ so that the PPC increases when $T(0)$ turns on, thereby causing more contraction of its target muscle group. Thus by (A1),

$$V(0) = 0, \tag{A3}$$

$$\frac{d}{dt}V(0) = \alpha(T(0) - P(0)) > 0. \tag{A4}$$

Consequently $V(t) \geq 0$ for all times t such that $0 \leq t \leq S$, where S is the first positive time, possibly infinite, at which $V(S) = 0$. While $V(t) \geq 0$ it follows by (A2) that

$$\frac{d}{dt}P = GV \tag{A5}$$

To solve equations (A1) and (A5), differentiate (A1) at times when $V(t) \geq 0$. Then

$$\frac{d^2}{dt^2}V = \alpha(-\frac{dV}{dt} - \frac{dP}{dt}), \tag{A6}$$

because T is constant. Substituting (A5) into (A6) yields the equation

$$\frac{d^2}{dt^2}V + \alpha\frac{d}{dt}V + \alpha GV = 0 \tag{A7}$$

subject to the initial data (A3) and (A4).

This equation can be solved by standard methods. The solution takes the form

$$V(t) = (T(0) - P(0))f(t), \tag{A8}$$

where $f(t)$ is independent of $T(0)$ and $P(0)$. Thus $V(t)$ equals the initial difference between the new TPC and the initial PPC multiplied by a function $f(t)$ which is independent of the new TPC and the initial PPC. By (A2),

$$\frac{d}{dt}P = (T(0) - P(0))g(t), \tag{A9}$$

where $g(t) = Gf(t)$. Integration of (A9) yields

$$P(t) = P(0) + (T(0) - P(0)) \int_0^t g(v)dv. \tag{A10}$$

Since $\frac{d}{dt}P$ provides an estimate of the arm's velocity profile, (A9) illustrates the property of duration invariance in the special case that $G(t)$ is constant. Duration invariance is proved using a general $G(t)$ in Appendix 2. Equation (A9) also illustrates how the velocity profile can respond to a sudden switch in the TPC with a gradual increase-then-decrease in its shape, although $g(t)$ assumes a different form if $\alpha > 4G$, $\alpha = 4G$, or $\alpha < 4G$. When $\alpha > 4G$,

$$g(t) = \frac{\alpha G}{\sqrt{\alpha^2 - 4\alpha G}} e^{-\frac{\alpha}{2}t}\left[e^{\frac{t}{2}\sqrt{\alpha^2 - 4\alpha G}} - e^{-\frac{t}{2}\sqrt{\alpha^2 - 4\alpha G}}\right]. \tag{A11}$$

Term $[\exp(\frac{t}{2}\sqrt{\alpha^2 - 4\alpha G})] - [\exp(-\frac{t}{2}\sqrt{\alpha^2 - 4\alpha G})]$ in (A11) increases exponentially from the value 0 at $t = 0$, whereas term $\exp[-\frac{\alpha}{2}t]$ decreases exponentially towards the value 0 at a faster rate. The net effect is a velocity function that increases-then-decreases with an approximately bell-shaped profile. In addition, $g(t) \geq 0$ and

$$\int_0^\infty g(t)dt = 1. \tag{A12}$$

By (A10) and (A12), $P(t)$ increases towards T as t increases. Thus $P(t)$ either approaches $T(0)$ with an arbitrarily small error, or an undershoot error occurs if the GO signal is switched off prematurely.

If $\alpha = 4G$, then

$$g(t) = \alpha G t e^{-\frac{\alpha}{2}t}. \tag{A13}$$

Again the velocity profile gradually increases-then-decreases, but starts to increase linearly before it decreases exponentially. The function in (A13) also satisfies (A12), so that accurate movement or undershoot occur, depending upon the duration of the GO signal.

The case of $\alpha < 4G$ deserves special attention. In this case, the rate G with which P is updated in equation (A2) exceeds the ability of the rate α in equation (A1) to keep up. As a result, an overshoot error can occur. In particular,

$$g(t) = \frac{2\alpha G}{\sqrt{4\alpha G - \alpha^2}} e^{-\frac{\alpha}{2}t} \sin\left(\frac{\sqrt{4\alpha G - \alpha^2}}{2} t\right) \tag{A14}$$

if $0 \leq t \leq \frac{2\pi}{\sqrt{4\alpha G - \alpha^2}}$. When t exceeds $\frac{2\pi}{\sqrt{4\alpha G - \alpha^2}}$, function $g(t)$, and thus $V(t)$, becomes negative. By (A2), $[V(t)]^+ = 0$ when t exceeds $\frac{2\pi}{\sqrt{4\alpha G - \alpha^2}}$, so that, by (A2), $P(t)$ stops moving at this time. The movement time in this case thus satisfies

$$MT = \frac{2\pi}{\sqrt{4\alpha G - \alpha^2}}. \tag{A15}$$

Within this time frame, the velocity profile is the symmetric function $\sin\left(\frac{\sqrt{4\alpha G - \alpha^2}}{2} t\right)$ multiplied by the decaying, hence asymmetric, function $e^{-\frac{\alpha}{2}t}$. Greater overall symmetry of $g(t)$ is achieved if the rate $\frac{\sqrt{4\alpha G - \alpha^2}}{2}$ with which the sine function changes is rapid relative to the rate $\frac{\alpha}{2}$ with which the exponential function changes; viz., if $2G \gg \alpha$.

Since $P(t)$ stops changing at time $t = \frac{2\pi}{\sqrt{4\alpha G - \alpha^2}}$, the final PPC value found from equation (A10) is

$$P\left(\frac{2\pi}{\sqrt{4\alpha G - \alpha^2}}\right) = P(0) + (T(0) - P(0))\left(1 + e^{-(\alpha\pi/\sqrt{4\alpha G - \alpha^2})}\right). \tag{A16}$$

Thus an overshoot error occurs of size

$$E = (T(0) - P(0))e^{-(\alpha\pi/\sqrt{4\alpha G - \alpha^2})} \tag{A17}$$

In accordance with Woodworth's Law, the error is proportional to the distance $(T(0) - P(0))$. Fitts' Law can be derived by holding E constant in (A17) and varying $(T(0) - P(0))$ to test the effect on the MT in (A15). Substituting (A15) into (A17) shows that

$$E = (T(0) - P(0))e^{-\frac{\alpha MT}{2}} \tag{A18}$$

which implies Fitts' Law

$$MT = \frac{2}{\alpha} \log\left(\frac{T(0) - P(0)}{E}\right). \tag{A19}$$

The initial condition $V(0) = 0$ in (A3) obtains if the system has actively tracked a constant TPC until its PPC attains this TPC value. Under other circumstances, $V(0)$ may be negative. When this occurs, $\frac{d}{dt}P$ in (A2) may remain 0 during an initial interval while $V(t)$ increases to nonnegative values. Thus P begins to change only after a staggered onset time. Some properties of staggered onset times are derived below.

A negative initial value of $V(0)$ may obtain if a particular muscle group has been passively moved to a new position either by an external force or by the prior active contraction of other muscle groups. In such a situation, $P(t)$ may be changed by the PUP circuit (Section 13.30) even if $T(t) = 0$, and $V(t)$ may track $P(t)$ via equation (A1) until a new equilibrium is reached. Under these circumstances, (A1) implies that

$$0 = \frac{d}{dt}V = \alpha(-V + 0 - P). \tag{A20}$$

If we assume that this equilibrium value obtains at time $t = 0$, then

$$V(0) = -P(0) < 0, \tag{A21}$$

and equation (A2) implies that

$$\frac{d}{dt}P = G[V]^+ = 0. \tag{A22}$$

Thus P remains constant until V becomes positive. If a new TPC is switched on at time $t = 0$ to an agonist muscle which satisfies (A21), then $T(0) > P(0)$. By (A1), V increases according to the equation

$$\frac{d}{dt}V + \alpha V = \alpha(T(0) - P(0)), \tag{A23}$$

where $\alpha(T(0) - P(0))$ is a positive constant, until the time $t = t_1$ at which $V(t_1) = 0$. Thereafter $[V]^+ = V > 0$ so that V and P mutually influence each other through equations (A1) and (A5).

Time t_1 is computed by integrating equation (A10). We find

$$V(t) = V(0)e^{-\alpha t} + (T(0) - P(0))(1 - e^{-\alpha t}) \tag{A24}$$

for $0 \leq t \leq t_1$. By (A21),

$$V(t) = -P(0) + T(0)(1 - e^{-\alpha t}). \tag{A25}$$

Thus

$$t_1 = \frac{1}{\alpha} ln \left[1 - \left(\frac{P(0)}{T(0)}\right)\right]^{-1}. \tag{A26}$$

By (A26), t_1 is a function of the ratio of the initial PPC value to the new TPC value.

For times $t \geq t_1$, equations (A1) and (A5) can be integrated just as they were in the preceding case. Indeed,

$$V(t_1) = 0 \tag{A27}$$

by the definition of t_1, and

$$\frac{d}{dt}V(t_1) = \alpha(T(0) - P(0)) \tag{A28}$$

by (A23) and (A28). The initial data (A27) and (A28) are the same as the initial data (A3) and (A4) except for a shift of t_1 time units. Consequently if the GO signal onset time is also shifted by t_1 time units, then it follows from (A8) that at times $t \geq t_1$,

$$V(t) = (T(0) - P(0))f(t - t_1). \tag{A29}$$

An estimate of such a velocity profile is found by piecing together (A24) and (A29). Thus

$$\frac{d}{dt}P = \begin{cases} 0 & \text{for } 0 \leq t < t_1 \\ G(T(0) - P(0))f(t - t_1) & \text{for } t_1 \leq t \end{cases} \tag{A30}$$

Equation (A30) illustrates how a velocity profile with a staggered onset time can occur if $V(0) < 0$. As shown in Section 13.26, the VITE command to a muscle group can compensate for a staggered onset time if its DV is multiplied by the same GO signal as other muscles in the synergy. In this case, the GO signal onset time is not shifted to match the onset time of each component of the VITE command.

APPENDIX 2

Synchrony and Duration Invariance

Consider equations (A1) and (A2) under the influence of an arbitrary nonnegative and continuous GO function $G(t)$. As in Appendix 1, let

$$V(0) = 0 \tag{A3}$$

and $P = T$ before T is switched to a new value. Suppose for definiteness that $T(t)$ switches from the value T_0 to T_1 at time $t = 0$, and that

$$T_1 > T_0 = P(0). \tag{A31}$$

Consequently, equations

$$\frac{d}{dt}V = \alpha(-V + T - P) \tag{A1}$$

and

$$\frac{d}{dt}P = GV \tag{A5}$$

hold for an interval of values $t \geq 0$. Define the new PPC variable

$$Q(t) = P(t) - T_0 \tag{A32}$$

and the new target position constant

$$T_2 = T_1 - T_0. \tag{A33}$$

Then (A1) and (A5) can be replaced by equations

$$\frac{d}{dt}V = \alpha(-V + T_2 - Q) \tag{A34}$$

and

$$\frac{d}{dt}Q = GV. \tag{A35}$$

By (A31),

$$Q(0) = 0. \tag{A36}$$

Thus by (A3) and (A36), both V and Q start out with 0 values at $t = 0$.

Now define new variables

$$v(t) = \frac{V(t)}{T_2} \tag{A37}$$

$$q(t) = \frac{Q(t)}{T_2}. \tag{A38}$$

By (A34) and (A35), these variables obey the equations

$$\frac{d}{dt}v = \alpha(-v + 1 - q) \tag{A39}$$

$$\frac{d}{dt}q = Gv. \tag{A40}$$

In addition,

$$v(0) = q(0) = 0 \tag{A41}$$

by (A3) and (A36). It is obvious that a unique solution of (A39)–(A41) obtains no matter how T_2 and T_1 are chosen, if $T_2 > T_1$.

By combining (A31), (A32), (A33), and (A38), we find that

$$P(t) = P(0) + (T_1 - P(0))q(t), \tag{A42}$$

where $q(t)$ is independent of T_1 and $P(0)$. Equation (A42) proves duration invariance given a general GO function $G(t)$. Indeed, differentiating (A42) yields

$$\frac{d}{dt}P = (T_1 - P(0))\frac{d}{dt}q(t) \tag{A43}$$

which shows that function $\frac{d}{dt}q$ generalizes function $g(t)$ in equation (A9).

APPENDIX 3

Passive Update of Position

Mathematical equations for a PUP circuit are described below. As in our description of a VITE circuit, equations for the control of a single muscle group will be described. Opponent interactions between agonist and antagonist muscles also exist and can easily be added once the main ideas are understood.

The PUP circuit supplements the equation

$$\frac{d}{dt}P = G[V]^+ \tag{A2}$$

whereby the PPC integrates DV's through time. A PUP circuit obeys equations

Present Position Command

$$\frac{d}{dt}P = G[V]^+ + G_p[M]^+, \tag{A44}$$

Outflow-Inflow Interface

$$\frac{d}{dt}M = -\beta M + \gamma I - zP, \tag{A45}$$

Adaptive Gain Control

$$\frac{d}{dt}z = \delta G_p(-\epsilon z + [M]^+). \tag{A46}$$

The match function M in (A45) rapidly computes a time-average of the difference between inflow (γI) and gated outflow (zP) signals. Thus

$$M \simeq \frac{1}{\beta}(\gamma I - zP). \tag{A47}$$

If the inflow signal γI exceeds the gated outflow signal zP, then $[M]^+ > 0$ in (A47). Otherwise $[M]^+ = 0$. The *passive gating function* G_p in (A44) is positive only when the muscle is in a passive, or postural, state. In particular, $G_p > 0$ only when the GO signal $G(t) \simeq 0$ in the VITE circuit. Figure 13.26 assumes that a signal $f(G(t))$ inhibits a tonically active source of the gating signal G_p. Thus G_p is the output from a "pauser" cell, which is a tonically active cell whose output is attenuated during an active movement. Such cells are well-known to occur in saccadic eye

movement circuits (Grossberg and Kuperstein, 1986; Luschei and Fuchs, 1972; Raybourn and Keller, 1977). If both G_p and $[M]^+$ are positive in (A44), then $\frac{d}{dt}P > 0$. Consequently, P increases until $M = 0$; that is, until the gated outflow signal zP equals the inflow signal zI. At such a time, the PPC is updated to match the position attained by the muscle during a passive movement. To see why this is true, we need to consider the role of function z in (A45) and (A46).

Function z is a long term memory (LTM) trace, or associative weight, which adaptively recalibrates the scale, or gain, of inflow signals until they are in the same scale as outflow signals. Using this mechanism, a match between inflow and outflow signals accurately encodes a correctly updated PPC. Adaptive recalibration proceeds as follows.

In equation (A46), the learning rate parameter δ is chosen to be a small constant to assure that z changes much more slowly than M or P. The passive gating function G_p also modulates learning, since z can change only at times when $G_p > 0$. At such times, term $-\epsilon z$ describes a very slow forgetting process which prevents z from getting stuck in mistakes. The forgetting process is much slower than the process whereby z grows when $[M]^+ > 0$. Since function M reacts quickly to its inputs γI and $-zP$, as in (A47), term $[M]^+ > 0$ only if

$$\gamma I > zP. \tag{A48}$$

The outflow signal P is multiplied, or gated, by z on its way to the match interface where M is computed (Figure 13.26).

Because z changes only when the muscle is in a postural, or a passive state, terms γI and P typically represent the same position, or state of contraction, of the muscle group. Then inequality (A48) says that the scale γI for measuring position I using inflow signals is larger than the scale zP for measuring the same position using outflow signals. When this happens, z increases until $M = 0$; viz., until outflow and inflow measurement scales are equal.

On an occasion when the arm is passively moved by an external force, the inflow signal γI may momentarily be greater than the outflow signal zP. Due to past learning, however, the inflow signal satisfies

$$\gamma I = zP^*, \tag{A49}$$

where P^* is the outflow command that is typically associated with I. Thus by (A47),

$$M \simeq \frac{z}{\beta}(P^* - P). \tag{A50}$$

By (A44) and (A50), P quickly increases until it equals P^*. Thus, after learning occurs, P approaches P^*, and M approaches 0 very quickly, so quickly that any spurious new learning which might have occurred due to the momentary mismatch created by the onset of the passive movement

has little opportunity to occur, since z changes slowly through time. What small deviations may occur tend to average out due to the combined action of the slow forgetting term $-\epsilon z$ in (A46) and opponent interactions.

Equations (A45) and (A46) use the same formal mechanisms as the *head-muscle interface* (HMI) described by Grossberg and Kuperstein (1986). The HMI adaptively recodes a visually activated target position coded in head coordinates into the same target position coded in agonist-antagonist muscle coordinates. Such a mechanism for adaptive matching of two measurement scales may be used quite widely in the nervous system. We therefore call all such systems Adaptive Vector Encoders.